University of Alberta

Development and Application of Real Time Cell Sensing Technique for Detection of Cytotoxicity Induced by Environmental Emerging Contaminants

by

Li Huang

A thesis submitted to the Faculty of Graduate Studies and Research in partial fulfillment of the requirements for the degree of

Master of Science

in

Environmental Health Sciences

Public Health Sciences

Edmonton, Alberta

Fall 2007

Library and Archives Canada

Published Heritage Branch

395 Wellington Street
Ottawa ON K1A 0N4
Canada

Bibliothèque et Archives Canada

Direction du Patrimoine de l'édition

395, rue Wellington
Ottawa ON K1A 0N4
Canada

Your file Votre référence
ISBN: 978-0-494-33262-7
Our file Notre référence
ISBN: 978-0-494-33262-7

NOTICE:
The author has granted a non-exclusive license allowing Library and Archives Canada to reproduce, publish, archive, preserve, conserve, communicate to the public by telecommunication or on the Internet, loan, distribute and sell theses worldwide, for commercial or non-commercial purposes, in microform, paper, electronic and/or any other formats.

The author retains copyright ownership and moral rights in this thesis. Neither the thesis nor substantial extracts from it may be printed or otherwise reproduced without the author's permission.

AVIS:
L'auteur a accordé une licence non exclusive permettant à la Bibliothèque et Archives Canada de reproduire, publier, archiver, sauvegarder, conserver, transmettre au public par télécommunication ou par l'Internet, prêter, distribuer et vendre des thèses partout dans le monde, à des fins commerciales ou autres, sur support microforme, papier, électronique et/ou autres formats.

L'auteur conserve la propriété du droit d'auteur et des droits moraux qui protège cette thèse. Ni la thèse ni des extraits substantiels de celle-ci ne doivent être imprimés ou autrement reproduits sans son autorisation.

In compliance with the Canadian Privacy Act some supporting forms may have been removed from this thesis.

While these forms may be included in the document page count, their removal does not represent any loss of content from the thesis.

Conformément à la loi canadienne sur la protection de la vie privée, quelques formulaires secondaires ont été enlevés de cette thèse.

Bien que ces formulaires aient inclus dans la pagination, il n'y aura aucun contenu manquant.

Canada

University of Alberta

Faculty of Graduate Studies and Research

The undersigned certify that they have read, and recommend to the Faculty of Graduate Studies and Research for acceptance, a thesis entitled Development and Application of Real Time Cell Sensing Technique for Detection of Cytotoxicity Induced by Environmental Emerging Contaminants and Particulate Matters submitted by **Li Huang** in partial fulfillment of the requirements for the degree of **Master of Science**.

Dr. Xingfang Li

Dr. Chris X. Le

Dr. Jonathan Martin

Dr. Jason Acker

Date approved: July 16, 2007

ABSTRACT

A novel technique for continuous and quantitative measurement of cytotoxicity using the cell-microelectronic sensing technology has been developed. This technique was used to test the cytotoxicity of four nitrosamines, N-nitrosodimethylamine (NDMA), N-nitrosodiphenylamine (NDPhA), N-nitrosopiperidine (NPip), and N-nitrosopyrrolidine (NPyr) on mammalian cells. Nitrosamines are a family of chemicals recently identified as disinfection by-products in drinking water. The unique cytotoxicity of NDPhA showing the most cytotoxic and cell cycle inhibition effect was observed for the first time.

This technique was further demonstrated for assessing the cytotoxicity of air particulate matter. The excellent signals without interference from particles provided a reliable measurement of cytotoxicity. Further studies demonstrated the different mechanisms underlying quartz particle induced cell death of two types of alveolar epithelial cells: necrosis for A549 cells (type II alveolar epithelial cells) and apoptosis for SKMES-1 cells (type I alveolar epithelial cells).

Acknowledgements

I would like to acknowledge a number of people for their help during my program. Firstly, I wish to express my sincerest gratitude to my supervisor Dr. Xing-Fang Li for her tremendous support and guidance throughout my program. I would like to express thanks to Ms. Li Xie, for being my great partner in conducting this whole project. I would also like to thank my lab mates for their feedback and discussions on my project. Without their constant encouragement and friendship, my graduate program would not have been the success that it was.

I would also like to take this opportunity to thank my family and friends for their love and support, especially my daughter at her age of only four, for her great understanding and support. Their love, caring and encouragement have made this work possible.

Thank you to everyone else, for seeing me through the challenges of graduate school!

CHAPTER 1: INTRODUCTION ---- 1

1.1 Drinking Water Disinfection and Disinfection By-Products ---- 1

1.2 Air Particulate Matter and Adverse Effects ---- 6

1.3 Cell Viability, Proliferation and Cytotoxicity ---- 7

1.3.1 Terminology of Cytotoxicity ---- 8

1.3.2 Apoptosis and Necrosis ---- 8

1.3.3 Apoptotic Pathways ---- 10

1.3.4 Regulation of the Cell Cycle ---- 12

1.4 Conventional Cytotoxicity Detection Techniques ---- 13

1.4.1 Permeability Assays ---- 14

1.4.2 Functional Assays ---- 15

1.4.3 Reproductive Assays ---- 15

1.5 New Cytotoxicity Detection Techniques—RT-CES System ---- 16

1.5.1 Introduction ---- 16

1.5.2 Instrumentation of RT-CES ---- 20

1.5.3 Principles and Validation ---- 21

1.6 Thesis Objectives ---- 24

1.7 References ---- 27

CHAPTER 2: DEVELOPMENT OF A CELL-MICROELECTRONIC SENSING TECHNIQUE FOR THE DETECTION OF CYTOTOXICITY OF NEWLY

DISCOVERED DISINFECTION BY-PRODUCTS AND CONSEQUENT

MECHANISTIC STUDY ---------- 322

2.1 Introduction ---------- 33

2.2 Materials and Methods ---------- 40

2.2.1 Chemicals and Media ---------- 40

2.2.2 Cell Culture and Growth Conditions ---------- 40

2.2.3 Calibration of Real-Time Cell Electronic Sensing System ---------- 40

2.2.4 Detection of Cytotoxicity of Four Nitrosamines on Four Different Cells ------ 41

2.2.5 Reversibility Study ---------- 43

2.2.6 Trypan Blue Stain Assay ---------- 43

2.2.7 Cell Cycle Analysis ---------- 44

2.3 Results and Discussion ---------- 44

2.3.1 Selection of Four In Vitro Models for Detecting the Cytotoxicity of DBPs. --- 44

2.3.2 Calibration Results of RT-CES for Four Cells ---------- 45

2.3.3 Cytotoxicity of Nitrosamines Determined by RT-CES Method ---------- 48

2.3.4 Cell Line Specific Cytotoxicity ---------- 55

2.3.5 Reversibility Study ---------- 56

2.3.6 The Effects of Cell-Killing and Cell Cycle Arrest of Nitrosamines on CHO Cells ---------- 59

2.4 References ---------- 65

CHAPTER 3: THE APPLICATION OF RT-CES SYSTEM ON CYTOTOXIC EFFECTS OF PULMONARY EPITHELIAL CELLS INDUCED BY PARTICULATE MATTERS AND MECHANISTIC STUDIES ---------- 67

3.1 Introduction ---------- 67

3.2 Materials and Methods ---------- 70

3.2.1 Cell Culture and Growth Conditions ---------- 70

3.2.2 Particals and Chemicals ---------- 70

3.2.3 Cytotoxicity Study Using the RT-CES System ---------- 71

3.2.4 Cell Cycle Analysis ---------- 73

3.2.5 Caspase Inhibitor Study ---------- 73

3.2.6 Electron Microscope Study ---------- 74

3.2.7 MMP Assay ---------- 75

3.3 Results ---------- 75

3.3.1 Linear Relationship Between the Cell Index and the Cell Number ---------- 75

3.3.2 Measurement of Cellular Response of A549 and SKMES-1 Cells After Quartz Particle Exposure ---------- 78

3.3.3 Corresponding Morphological Changes Implicated by RT-CES Results. ------ 84

3.3.4 Involvement of Caspases Evidenced by the Protective Effects of Caspase Inhibitor ---------- 91

3.3.5 Quartz-Induced Early MMP Change in SK-MES-1 Cells ---------- 93

3.3.6 Application of the RT-CES Technique in Biomonitoring the Cytotoxicity of Different Particles ---- 94

3.4 Discussion ---- **100**

3.5 References ---- **108**

CHAPTER 4: SUMMARY AND FUTURE WORK ---- **111**

LIST OF FIGURES

Figure 1-1 Relative percentage of halogenated DBPs speices as a proportion of TOX in chlorinated drinking water 4

Figure 1-2 Relative percentage of specific AOC species to total AOC in ozonated drinking water.....4

Figure 1-3 The extrinsic and intrinsic apoptotic pathways.....12

Figure 1-4 Components of RT-CES system.....21

Figure 1-5 The E-plate and circle-on-line microelectrode array technique.....21

Figure 2-1 Calibration curves of different cell lines and the correlations between the CI obtained from RT-CES and the cell number.....47

Figure 2-2 The responses of CHO-K1, A549, T24, $HepG_2$ cells towards NDMA exposure.....49

Figure 2-3 The responses of CHO-K1, A549, T24, $HepG_2$ cells towards Npyr exposure.....50

Figure 2-4 The responses of CHO-K1, A549, T24, $HepG_2$ cells towards Npip exposure. 51

Figure 2-5 The responses of CHO-K1, A549, T24, $HepG_2$ cells towards NDPhA exposure..... 52

Figure 2-6 Comparison of IC_{50}s at 24 h of four nitrosamines on four cell lines.....53

Figure 2-7 Reversibility study results of nitrosamines on CHO cells and A549 cells.....58

Figure 2-8 Cell death percentage in CHO-K1 cells treated with four nitrosamines.....60

Figure2-9 Cell cycle analysis of CHO cells after treatment of four nitrosamines.....61

Figure3-1 Cell quantification on the RT-CES system.....77

Figure 3-2 Dynamic monitoring of cytotoxic responses of A549 and SKMES-1 cells in response to quartz particles..... 80

Figure 3-3 The interference of particles on acid phosphatise assay.....82

Figure 3-4 The interference from particles in the RT-CES method.....83

Figure 3-5 Corresponding morphological changes observed from scanning electron microscopic study..... 85

Figure 3-6 Subseqnent flow cytometry study indicating the different mechanisms underlying different quartz induced A549 and SKMES-1 cytotoxicity....88

Figure 3-7 Transmission electron microscopic study results.....90

Figure 3-8 Results of viability assay comparing the protective effects of pan-caspase inhibitor from quartz induced cell death..... 92

Figure 3-9 Cell cycle analysis results detecting the decrease of apoptosis cells after pre-treatment with caspase inhibitor..... 92

Figure 3-10 Results of MMP test evaluating mitochondrial damage which is an indicator of intrinsic apoptotic pathway. 94

Figure 3-11 Cytotoxic effects of four particles on A549 cells.....96

Figure 3-12 Effects of quartz Q66, quartz Q70, SRM 1649a, SRM 2975 on SKMES-1 cells..... 97

Figure 3-13 Results of dose-response analysis for particle induced cytotoxicity on SK-

MES-1 cells.....98

LIST OF TABLES

Table 1-1	Comparison of previous studies on ECIS technique	18
Table 2-1	N-Nitrosamine Species investigated.	39
Table2-2	Nitrosamine cytotoxicity results on four cell lines	54
Table 2-3	Summary of cytotoxicity of nitrosamines on CHO cells and the mechanistic information obtained from this study	63

LIST OF ABBREVIATIONS

AChE	Acetylcholinesterase
AEC	Alveolar Epithelial Cells
Apaf-1	Apoptotic Protease-Activating Factor-1
AOC	Assimilable Organic Carbon
Bax	Bcl-2–Associated X Protein
Bak	Bcl-2 Antagonist/Killer
Bcl-2	B-Cell Lymphoma Gene 2
BDCM	Bromodichloromethane
Caspase	Cysteinyl Aspartate-Specific Protease
CD95	Cluster of Differentiation Antigen 95
CDBM	Chlorodibromomethane
CDK	Cyclin Dependent Kinase
CI	Cell Index
CYP	Cytochrome P450
DISC	Death Inducing Signaling Complex
DCAA	Dichloroacetic Acid
DBAA	Dibromoacetic Acid
DBP	Disinfection By-Product
DEP	Diesel Exhaust Particle
DHS	Department of Health Services

DMA	Dimethylamine
DMEM	Dulbecco's Modified Eagle Media
DON	Dissolved Organic Nitrogen
ECIS	Electrical Cell-substrate Impedance Sensing
FADD	Fas-Associated Death Domain
Fas	FS7-associated surface antigen (apo-1)
FasL	Fas ligand
HAA	Haloacetic Acid
IMAC	Interim Maximum Acceptable Concentration
IRIS	Integrated Risk Information System
JC-1	5,5',6,6'-tetrachloro-1,1',3,3'-tetraethylbenzimidazolcarbocyanine iodide
LDH	Lactase Dehydrogenase
MCL	Maximum Contaminant Level
MOE	Ministry of the Envrionment
MTT	3-(4,5-dimethylthiazol-2-yl)-2,5-diphenyltetrazoliumbromide
MMP	Mitochondria Membrane Potential
NADH	Nicotinamide Adenine Dinucleotide
NDMA	N-nitrosodimethylamine
NDPhA	N-nitrosodiphenylamine
NPip	N-nitrosopiperidine
NPyr	N-nitrosopyrrolidine

NOM	Natural Organic Matter
NCI	National Cancer Institute
NIEHS	National Institute of Environmental Health Sciences
NIST	National Institute of Standards and Technology
NRU	Neutral Red Uptake
PAH	Polycyclic Aromatic Hydrocarbon
PCB	Polychlorinated Biphenyl
PI	Propidium Iodide
PM	Particulate Matter
RC	Registry of Cytotoxicity
RT-CES	Real-Time Cell Microelectronic Sensing
SEM	Scanning Electron Microscope
SRM	Standard Reference Materials
TEM	Transmission Electron Microscope
THM	Trihalomethane
TTHM	Total Trihalomethane
TOX	Total Organic Halide
UDMH	Unsymmetrical Dimethylhydrazine
UFP	Ultrafine Particle

:

:

1 Chapter 1: Introduction

My thesis research involves several components including (1) development of a real-time cell microelectronic sensing (RT-CES) method for high throughput testing of chemical toxicity; (2) application of the RT-CES method to detect the cytotoxicity of nitrosamines, a family of emerging drinking water disinfection by-products (DBPs); (3) development and application of the RT-CES technique to examine cellular responses to air particulate matter. Background information on a number of research areas is important to help understanding the proposed research in this thesis. Chapter one will review briefly (1) drinking water disinfection and unintended by-product formation, characterization, toxicity, and health concerns, (2) air particulates and health effects, and (3) in vitro toxicity testing technologies for the examination of the toxicity of chemicals and particulates.

1.1 Drinking Water Disinfection and Disinfection By-Products

Drinking water disinfection is one of the most successful public health measures to eliminate or reduce waterborne microbial diseases. Drinking water disinfection techniques include the use of chemical disinfectants such as chlorine, chloramines, chlorine dioxide, hypochloride, ozone, or the combination of both chemical disinfection and UV treatment (Cantor 1997). However, the disinfection processes can unintentionally result in the formation of disinfection by-products (DBPs) in finished drinking water.

Disinfectants, such as chlorine, chlorine dioxide, hypochlorite, chloramines, and ozone, can react with natural organic matter in the water, such as humic and fulvic acids to generate some unintended by-products (Cantor 1997).

The first identification of chloroform as a DBP in chlorinated drinking water in 1974 led to the United States Environmental Protection Agency (US EPA) survey of DBPs in 1976. It was found that chloroform and other trihalomethanes (THMs) commonly existed in chlorinated drinking water (Rook, 1974; Kopfler et al. 1976). In addition, the US National Cancer Institute (NCI) found an association between chloroform exposure and various cancers in laboratory animals (NCI report, 1976). These studies reached the consensus that the DBPs issue is an important public health and regulatory concern. The first regulation was issued in 1979 by the US EPA to control the total THMs (TTHMs) below 0.1 mg/L (ppb) in finished drinking water (EPA document, 2003), and the Stage 1 Disinfectants/Disinfection By-Products (D/DBP) Rule, which requires reducing the maximal contaminant level of THMs to 0.08 mg/L and regulates five haloacetic acids, bromate, and chlorite for the first time, became effective on January 1, 2002 (National Primary Drinking Water Regulations, 1998). In Canada, the Canadian Drinking Water Guidelines regulated the levels of THMs and bromodichloromethane (BDCM) to 0.1 and 0.16 mg/L, respectively, but no other DBPs have been regulated in Canada (Health Canada 2006).

To date, more than 500 DBPs have been identified in drinking water (Richardson,

Simmons et al. 2002). However, there are many more unidentified DBP species with unknown toxicity information. It was shown that there are still more than 60% unidentified species both in total organic halide (TOX) in chlorinated water (Figure 1-1) and assimilable organic carbon (AOC) compounds in ozonated water (Figure 1-2) (Richardson, Simmons et al. 2002). TOX and AOC represent only some types of DBPs formed in drinking water, and the percentage of unidentified DBPs is much higher. Today, alternative disinfectants, such as ozone, chlorine dioxide, and chloramines, are utilized extensively in many drinking water utilities to minimize the concentration of regulated THMs and haloacetic acids (HAAs). However, the switch from chlorination to other disinfection processes may create unregulated and unmonitored DBPs. For example, ozonation can generate much more bromate when the source water contains elevated bromide levels (Simmons, Teuschler et al. 2004). Those unregulated and unidentified DBPs whose toxicity information is unknown or unavailable may pose a greater threat to public health. Thus, further work is needed to obtain crucial information regarding the toxicity, formation, and exposure assessment of DBPs.

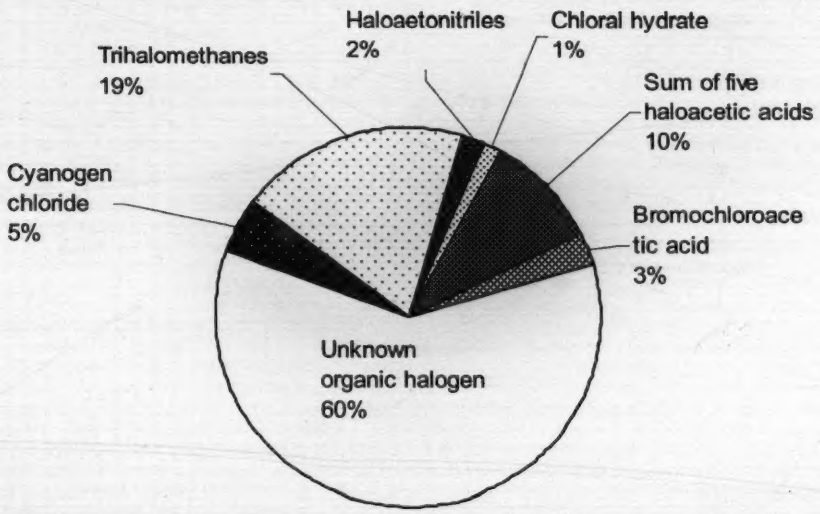

Figure1-1 Relative percentage of halogenated DBPs species as a proportion of TOX in chlorinated drinking water. Adapted from Richardson et al. (Richardson, Simmons et al. 2002).

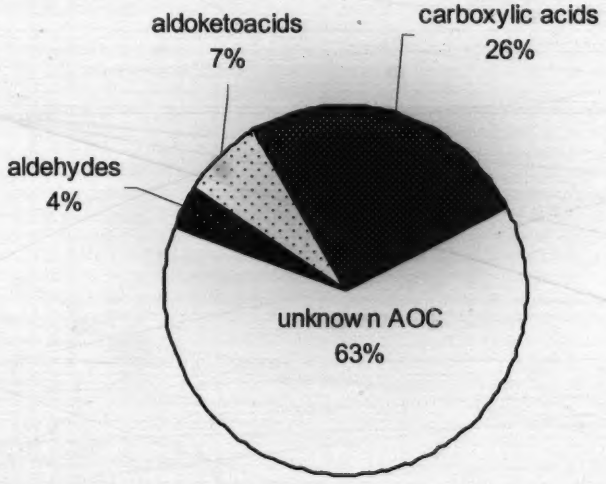

Figure 1-2 Relative percentage of specific AOC species to total AOC in ozonated drinking water. Adapted from Richardson et al. (Richardson, Simmons et al. 2002)

Numerous epidemiological and toxicological studies have associated the consumption of chlorinated drinking water with increased cancer incidence in various vital organs (Cantor 1997; Cantor, Lynch et al. 1998; Boorman 1999; McDorman, Pachkowski et al. 2005). The association of disinfection by-products and bladder cancer is strongest while increased risk of either colon or rectal cancer was also observed but not consistently (Cantor 1997). Consumption of drinking water with high levels of DBPs has also been associated with adverse reproductive outcomes such as spontaneous abortion (Swan, Waller et al. 1998; Waller, Swan et al. 1998), intrauterine growth retardation (Kramer, Lynch et al. 1992; Nuckols, Ashley et al. 2005), low birth weight (Gallagher, Nuckols et al. 1998; Nuckols, Ashley et al. 2005), and very preterm and preterm births (Nuckols, Ashley et al. 2005). Immunotoxicity of DBPs (Mather, Exon et al. 1990; French, Copeland et al. 1998; French, Copeland et al. 1999; Guo, McCay et al. 2001; Karrow, Guo et al. 2001), neurotoxicity of DCAA (Moser, Phillips et al. 1999), and the effect of DBAA on the reproductive competence and sperm quality (Linder, Klinefelter et al. 1995) were also reported.

1.2 Air Particulate Matter and Adverse Effects

Air particulate matter is referred to as particles, dust, dirt, soot, and aerosol mists that are suspended in the surrounding air. It may consist of solids of various forms including fibers or liquids (Gillissen, Gessner et al. 2006). Airborne particulate matter is a worldwide environmental and public health concern because the exposure of PM is associated with a series of adverse health effects (Glinianaia, Rankin et al. 2004; Brunekreef and Forsberg 2005; Gao, Yu et al. 2005). The impact on public health associated with particulate matter includes: (1) respiratory disorders and diseases such as pulmonary function disorder, respiratory syndromes, lung growth impairment, chronic obstructive pulmonary diseases, and lung cancer (Annesi-Maesano and Dab 2006; Gillissen, Gessner et al. 2006), (2) cardiovascular morbidity and mortality (Brook 2005), (3) developing fetus impact (Glinianaia, Rankin et al. 2004) and (4) immunotoxicity and allergic diseases (Heinrich and Wichmann 2004; Huang and Xu 2004).

Chemical and toxicological characterization of particulate matter in ambient air is difficult because its complex composition varies temporally and spatially and because it has diverse chemical and toxicological properties. Several studies have reported the examination of the toxicity of fractionated local air particulates (Hsiao, Mo et al. 2000; Muller, Wichmann et al. 2006). This approach is useful for addressing the problems related to chemical and toxicological characterization of local air pollutants; however, it is hardly possible to conduct interlaboratory studies with this approach. Air particulate

matter standard reference materials (SRM) are a practical way to study uniformly the adverse effects of particulate matter. The US National Institute of Standards and Technology (NIST) has developed several SRMs of air particulate matter since the early 1980s. SRM 1649a is an urban dust mixture that contains 120 components, 44 or more PAHs, 29 polychlorobiphenyl (PCB) congeners, chlorinated pesticides, and inorganic constituents (Musafia-Jeknic, Mahadevan et al. 2005). SRM 2975 is a diesel exhaust particles (DEP) mixture derived from a forklift with a heavy-duty diesel engine. DEP is a complex mixture of particles (< 1.0 μm in diameter) and combustion gas. These particles have organic compounds adsorbed on an elemental carbon core that may be inhaled deeply into the lungs. According to the US EPA health assessment document in 2002, long-term exposure to DEP is likely to pose a risk of lung cancer as well as damage the lung in other ways depending on exposure, while short-term exposure can cause transient irritation and inflammatory symptoms.

1.3 Cell Viability, Proliferation, and Cytotoxicity

Currently, the generation of large amount of anthropogenic or natural contaminant chemicals leads to an increasing demand for appropriate regulation based on toxicity information. In vivo toxicological studies usually need large numbers of experimental animals so that often associated with high cost and ethical issues. With the development of cell culture and other molecular biological techniques becoming available, rapid in vitro cytotoxicity tests became practical prescreening tools in toxicological study because

of the advantages such as low cost, uniform experimental condition, simplified maneuver procedures, etc.. The cytotoxicity information could be used to rank and prioritize the relative toxicity of relevant compounds with the combination of an array of other examination methods. Those in vitro assays also can provide mechanistic information such as chemical's binding to proteins, DNA damages, cell death pathways, etc.

1.3.1 Terminology of Cytotoxicity

Cell death is defined as the termination of the cell's ability to conduct vital functions such as metabolism, growth, reproduction, responsiveness, and adaptability (PubMed MeSH). The definitions of cytotoxicity are diverse and depend on which end point the researchers choose to examine; this can influence strongly the choice of specific assays and the interpretation of experimental results (Cook and Mitchell 1989). Different laboratories have a tendency to favor different assays and derive different terms such as viability, cell survival, cell killing, irreversible cell injury, and cytotoxicity (Acosta, Daniel, 2001). Currently, the consensus criteria for cytotoxicity assessment are still being defined.

1.3.2 Apoptosis and Necrosis

Cell death can occur by necrosis or apoptosis or both. Necrosis, an "accidental" cell death mode, is a pathological cell death process when cells are exposed to serious chemical or physical insult (Lecoeur, Prevost et al. 2001). Apoptosis, a "programmed"

cell death mode, is an important physiological process by which damaged or senile cells are eliminated without triggering inflammation (Formigli, Conti et al. 2004).

The term "apoptosis" was introduced by Kerr in 1972 to describe a particular form of cell death in which cells commit suicide by breaking themselves into membrane-bound apoptotic bodies (Kerr, Wyllie et al. 1972). Apoptosis allows multicellular organisms to remove old or damaged cells in a protective process that is distinct from necrosis (Kerr, Wyllie et al. 1972). Necrosis results in irreversible swelling of the cytoplasm and organelles followed by eventual lysis and release of its contents to its surroundings (Fadeel, Orrenius et al. 1999). The release of cellular components affects neighboring cells and can potentially cause a damaging inflammatory response. Necrosis typically occurs when cells are exposed to traumatic conditions such as hypoxia, ischemia, hyperthermia, and metabolic toxins as well as following direct cell trauma (Kerr, Wyllie et al. 1972). Unlike necrosis, apoptosis is morphologically characterized by chromatin condensation and fragmentation, cell shrinkage, and membrane blebbing (Kerr, Wyllie et al. 1972; Arends and Wyllie 1991; Takahashi and Earnshaw 1996). Changes in the plasma membrane composition during apoptosis signal phagocytes to absorb the apoptotic cell without provoking a generalized inflammatory response (Arends and Wyllie 1991; Takahashi and Earnshaw 1996).

Apoptosis is an important physiological event that is required for normal cell development as well as for controlling pathological processes (Kerr, Wyllie et al. 1972).

Because of its importance, apoptosis is a tightly regulated process, and hence any abrogation of the normal apoptotic regulation can lead to a number of diseases (Fadeel, Orrenius et al. 1999). For example, accumulation of uncontrolled cells due to insufficient apoptosis can lead to cancer, and cell loss due to excessive apoptosis results in stroke, neurodegeneration, lung disease, and heart failure (Fadeel, Orrenius et al. 1999).

1.3.3 Apoptotic Pathways

There are two distinct pathways through which apoptosis can occur: the death receptor mediated extrinsic apoptotic pathway and the mitochondria initiated intrinsic pathway. Caspases, a family of cysteinyl aspartate-specific proteases, are central mediators of both the extrinsic and the intrinsic apoptotic pathway. Caspases are synthesized as zymogens with a prodomain of variable length followed by a large subunit (p20) and small subunit (p10). These prodomains allow recruitment and activation in protein complexes through proteolysis at specific Asp residues residing between the prodomains; the p20 and p10 subunits then exert catalytic functions (Walczak and Krammer 2000).

In death receptor-mediated apoptosis, ligands such as CD95/Fas/APO-1 induce receptor trimerization and formation of a death inducing signaling complex (DISC) (Walczak and Krammer 2000; Walczak and Sprick 2001). This complex, located at the cell membrane, then recruits procaspase-8 via the FADD adaptor molecule (Muzio, Chinnaiyan et al. 1996) and induces a conformational change in procaspase-8, which

results in caspase cleavage and activation (Muzio, Chinnaiyan et al. 1996; Walczak and Krammer 2000; Walczak and Sprick 2001). Caspase-8, as an initiator caspase, can then activate directly or indirectly executive caspases, such as capase-3.

Some other apoptogenic agents induce apoptosis by disrupting the membrane integrity of mitochondria, which release proteins that initiate and promote caspase activation catalysed by the apoptosome complex (Cain, Brown et al. 1999; Saleh, Srinivasula et al. 1999; Zou, Li et al. 1999). Release of cytochrome c from the mitochondria provides the signal for the initiation of the assembly of the large multi-subunit apoptosome complex. Once assembled, the apoptosome recruits and activates caspase-9 which remains bound to Apaf-1 to form a holo-enzyme complex that activates the downstream effector, caspase-3 (Bratton, Walker et al. 2001). A large number of modulation proteins, such as Bcl-2, Bcl-X_L, and Bax/Bak, are actively involved in the intrinsic apoptotic pathway by promoting or inhibiting certain steps. Figure 1-3 summarizes these two distinct pathways.

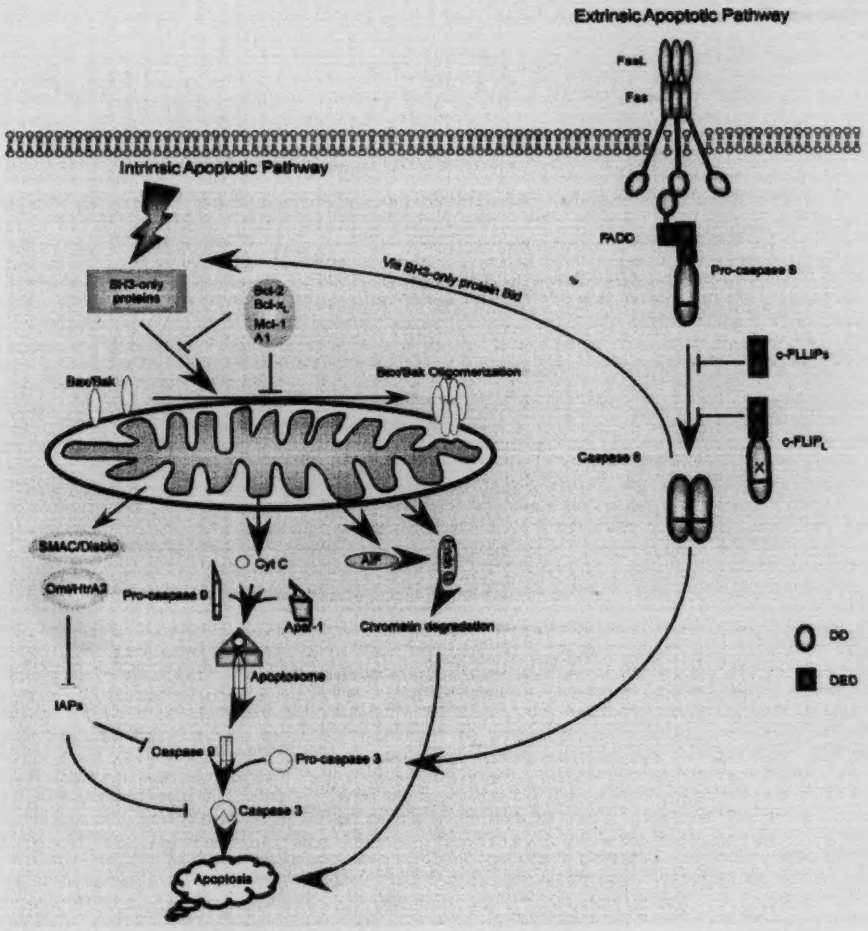

Figure 1-3. The extrinsic and intrinsic apoptotic pathways.

http://www.cell-research.com/200510/figs/img/749_fig01.gif

1.3.4 Regulation of the Cell Cycle

Eukaryotic cells replicate themselves through a well-regulated cell cycle process during which the cell duplicates its chromosomes and each copy of the chromosome is

segregated into a daughter cell. Precise and strict regulation of the cell cycle is crucial for normal development of multicellular organisms and high fidelity passage of cells. Disturbance of the cell cycle will result in severe consequences such as chromosome mis-segregation (aneuploidy), failure of DNA repair, accumulation of DNA damage, and subsequent generation of tumors (Luch 2002).

The cell cycle consists of four different phases with different functions: G0/G1, S (synthesis), G2, and M (mitosis) phase; mitosis can be further subdivided into four phases, prophase, metaphase, anaphase, and telophase. The period between two consecutive M phases is referred to as interphase which equals the sum of G0/G1, S, and G2 phases (Baserga 1965). This process is strictly regulated by a number of cell cycle checkpoints which are controlled by CDK/cyclin complexes and regulated by other relevant kinase inhibitors, subunit phosphorylation, or binding to CDKs (Wainwright, Lasorella et al. 2001). For example, cyclin D-CDK4/6 complexes function early for the cells entering from G1 phase to S phase. Inhibition of cyclin D dependent activity of CDK4 and CDK 6 by specific chemical inhibitors consequently results in arrest of the cell cycle in G1 phase. On the contrary, overexpression of cyclin D or lack of endogenous CDK inhibitors not only elevate the cell proliferation rate but may also contribute to carcinogenesis (Luch 2002).

1.4 Conventional Cytotoxicity Detection Techniques

In vitro cytotoxicity assays measure the extent to which a toxicant is cytotoxic to

cells by measuring various parameters of a population of cells. Cytotoxicity can be assessed by detecting the integrity of the cell membrane, the change of metabolic markers or membrane markers. We reviewed several conventional cytotoxicity assays in terms of its principles, advantages and disadvantages.

1.4.1 Permeability Assays

A damaged cell membrane will allow large molecules which are normally excluded by cells entering into the cytosome. Thus, if we introduce large molecules with specific light-absorbing or fluorescent properties, we can identify the dead cells from live cells. Trypan blue assay is an example (Fong and Kissmeyer-Nielsen 1972). Damaged cells stain dark blue, whereas undamaged cells appear translucent under the light microscope. Fluorescent dyes, such as propidium iodide, make the cells appear fluorescent as the dye enter the membrane and bind to nucleic acids (Diaz, Manez et al. 2003).

Permeability assays also include some methods that can detect the release of intracellular enzymes such as lactate dehydrogenase from the treated cells, for example, LDH assay. This assay is to measure the activity of dehydrogenase in cell supernatant fluids to correlate with cell viability (Decker and Lohmann-Matthes 1988).

The main disadvantage of dye permeability assays is that membrane damage may be a late event comparing to other organelles damage (John A. Cook 1989) so that these assays tend to underestimate cytotoxicity.

1.4.2 Functional Assays

Functional assays are another type of viability assay which examine the cell's metabolic properties that are essential for maintenance of normal function. For example, the MTT assay is the most frequently used functional assay and it detects the amount of succinate dehydrogenase by using a tetrazolium dye. This dye serves as a hydrogen acceptor and is reduced to formazan products which can be measured at 565 nm (Stratford and Stephens 1989). Disadvantages of this method include the different time periods required for staining different cell types (Cook and Mitchell 1989). Another limitation is associated with colorimetric assay, the color of chemicals to be tested will interfere with the readout, especially in the case of testing particulate matters because particles are usually dark and unable to be dissolved.

1.4.3 Reproductive Assays

Colony formation assays is major reproductive assay which measures the ability of cells to proliferate as indicator of viable status. Known numbers of single cells in a mixture of growth medium and agarose are poured onto petri dish to form soft agar. Each single cell will subsequently replicate itself and form a colony eventually (Byfield, Weintraub et al. 1973). Hence, if 100 cells were inoculated, then 90 colonies formed later indicate 90 % survival.

The main disadvantages include the long incubation time required. Formation of visible colonies takes 2.5 to 3 weeks even for fast-growing human tumor cell lines. In

addition, this method could not differentiate cells arrested by cytostatic toxicants from dead cells (Cook and Mitchell 1989).

Taken together, in all of those conventional cytotoxicity detection methods it is almost impossible to control the quality of cells, which is usually reflected in cell growth rates and growth patterns. In addition, the multiple procedures involved may generate systematic errors and affect the experimental results in an unpredictable manner. By realizing these disadvantages, researchers found that a real-time, dynamic cell biological response monitoring technique is needed.

1.5 New Cytotoxicity Detection Techniques—RT-CES System

1.5.1 Introduction

In 1984, Giaever and Keese first reported the application of Electrical Cell-substrate Impedance Sensing (ECIS) for real-time monitoring of cellular biological status (Giaever and Keese 1984). This totally non-invasive, label-free technique met the needs of researchers working on in vitro cellular experiments to monitor the response of cells without interference in real time, and it became a new focus of researchers. The cells were cultured in a well embedded with specially designed gold electrodes and were subjected to an external electrical field. When the cells attached to the electrodes, the impedance between the electrodes and the surrounding medium buffer solution was increased. The changes in impedance were measured continuously and quantitatively to reflect the changes in viability and morphology of the cells (Giaever and Keese 1984).

The ECIS technique provides a less labor-intensive way to observe dynamic cellular biological changes in a real-time manner. This method is the least invasive without using any other labeling techniques such as fluorescence, radioisotopes, etc.

Over the last 20 years, several reports described the use of ECIS technology (Applied Biophysics) to monitor cellular events, including epithelial cell-matrix attachment (Gailit and Clark 1996; Ramirez-Icaza, Mohammed et al. 2004), cell movement and spreading (Giaever and Keese 1984; Pei, Keese et al. 1994), the endothelial response under fluid shear stress (DePaola, Phelps et al. 2001), the alteration of the barrier function of bronchial epithelial cells after antigen exposure (Antony, Tepper et al. 2002), and the study of the capacity of Acetylcholinesterase (AChE) to increase the cell-substratum adhesion (Sharma, Koenigsberger et al. 2001). The size and disposition of the electrodes were altered to achieve better sensitivity and accuracy by other researchers; a few characteristics of their methods and their application to each study are shown in Table 1-1.

Table 1-1. Comparison of previous studies on ECIS technique.

Author	ZhengDong Pei et al., 1994	Depaola et al., 2001	Giaever et al., 1984	Antony et al., 2002	Xiao et al., 2002
Detection Electrode size	10^{-3} cm^2*4	5*10^{-4} cm^2* 8	3*10^{-4} cm^2* 4	10^{-4} cm^2* 10	0.057 mm^2
Well Size	60 mm	38 mm* 75 mm	60 mm	1 cm^2	0.9mm *0.9 mm
The area ratio (electrode/well)	1/10000	--	--	1/1000	---
Seeding cell number	Not available	2*10^5 cells/cm^2	10^5 cells/cm^2	10^5 cells/cm^2	5*10^4 cells
Application	Cell spreading and cell motion	Endothelial morphology and function change	To observe the cell morphology and the cell density	Measurement of BEAC permeability	To study the cytotoxicity

In the classic ECIS system (Giaever and Keese 1984; Xiao, Lachance et al. 2002), one large-area reference electrode and one small detection gold electrode (for example, with a surface area of 0.057 mm^2, compared with the well bottom surface area of 100

mm^2) are incorporated into the bottom of a cell-culture well. Usually, 50,000 cells were inoculated into the well and the resistance measured as the readout depended on the resistance between the detection electrodes and the reference electrodes (Xiao, Lachance et al. 2002). However, the detection electrode can sustain only 896 cells at most if we calculate that the typical cell is 9 μm in diameter or even less when the cells spread and reach larger dimensions. This means that only the response of less than 1% of the total cells were measured and recorded. Thus, the readout resistance could be largely variable from well to well if the cells present uneven distribution patterns. The short observation period of 24 h limits the application of this system to explore other important cytotoxic characteristics such as reversibility and the cytotoxic effects of repetitive administration of toxicants. Also, because a large amount of cells must be inoculated to overcome the high well-to-well variability, the dynamic range of this technique is relatively low (Solly, Wang et al. 2004). Here, we have applied a real-time cell electronic sensing (RT-CES™) (ACEA Biosciences Inc., San Diego, CA) system for cell-based cytotoxicity screening assays. The uniquely designed circle-on-line microelectrode array covers more than 80% of the bottom area of each well and allows the monitoring of nearly all the cells present in the wells, resulting in reliable and reproducible measurement of biological responses (Xing, Zhu et al. 2005).

1.5.2 Instrumentation of RT-CES

As shown in Figure 1-3, the RT-CES system consists of the following components: the sensor analyzer, the integrated software, the device station, and the 16-well E-plate. The core of the system is the circle-on-line microelectronic sensor arrays (Figure 1-4) that are integrated onto the bottom of the microwells on the E-plate. The device station could accommodate at most six E-plates at one time. The sensors provide continuous quantitative information concerning the biological status of the cells present in each well. The E-plate station is placed inside the CO_2 incubator and connected to the sensor analyzer. The data are collected and recorded automatically by the sensor analyzer under the control of the integrated software.

Figure 1-4. Components of the RT-CES system.

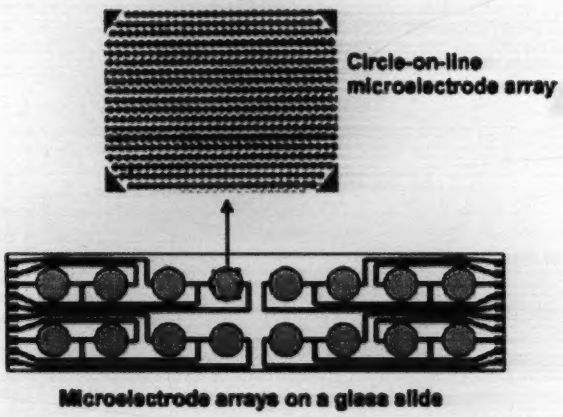

Figure 1-5. The E-plate and circle-on-line microelectrode array technique. Adapted from Xing et al., 2004.

1.5.3 Principles and Validation

The basic principles of the RT-CES system is to monitor the changes in electrode impedance induced by the interaction between testing cells and electrodes (Solly, Wang et al. 2004). When no cells are present on the electrodes, the total electronic impedance

consists of the resistance of the electrolyte solution and the impedance at the electrode/solution interface; when cells are present between the electrodes and the surrounding solution, the impedance consists of three parts: the resistance of the electrolyte solution, the cell impedance modeled as a resistance and a capacitance in parallel, and the impedance at the electrode/cell and electrode/solution interface (Solly, Wang et al. 2004).

Upon the application of an electrical field, ions undergo concentration-gradient-driven diffusion, leading to frequency dependent-impedance dispersion. The presence of the cells will increase the electrode impedance that could be monitored with RT-CES system (Solly, Wang et al. 2004).

The cell index (CI) is an arbitrary parameter of the status of cells present based on the electrical impedance measured. The equation of CI is:

$$\mathrm{CI}=\max_{i=1.....N}\left(\frac{R_{cell}(f_i)}{R_b(f_i)}-1\right),$$

where $R_b(f)$ and $R_{cell}(f)$ are the frequency-dependent electrode impedance without cells and with cells present, respectively(Xing, Zhu et al. 2005);N represents the number of the frequency points measured (N=3 for 10 kHz, 25 kHz, and 50 kHz). Thus, CI is a quantitative measurement that reflects the cellular response from two perspectives: first, under the same physical conditions, the CI value is proportional to the number of cells attached to the electronic sensor; the larger the CI value, the more cells attached to the

electronic sensor. Second, even when the same number of cells attach to the electronic sensor, depending on the cellular morphological changes such as cellular rounding, cell spread and the change of the status of adhesion and detachment, the CI value would increase or decrease accordingly. (Xing, Zhu et al. 2006). Since 2004, the first launch of RT-CES, this technique has been widely applied to fast cytotoxicity screening of environmental chemicals (Xing, Zhu et al. 2005), evaluation of the anti-tumor effects of various drugs, dynamic monitoring of the cell adhesion and spreading in response to different extracellular matrix proteins (Atienza, Zhu et al. 2005), detection of natural killer T-cell induced cytotoxicity and cell adhesion change (Glamann and Hansen 2006), assessment of the different function of G-protein-coupled receptor (GPCR) (Nuckols, Ashley et al. 2005), and screening, identifying, and characterizing receptor tyrokine kinase inhibitor from a compound library (Atienza, Zhu et al. 2005).

The validity of RT-CES as a reliable screening method for acute cytotoxicity has been evaluated by few studies (Solly, Wang et al. 2004; Xing, Zhu et al. 2006; Zhu, Wang et al. 2006). In these studies, researchers compared the RT-CES method with the Cell Titer Glo™ assay (Premega), the NRU test, and the MTT assay and demonstrated good correlations between RT-CES and other methods. In addition, with respect to the registry of cytotoxicity (RC) prediction model, which is a recommended evaluation tool for candidate cytotoxicity assay, the RT-CES results met the accepted requirements, according to NIH publication #01-4500, and predicted acute toxicity accurately when

evaluated by this prediction model (Xing, Zhu et al. 2006).

To date, more than 100 cell lines have been tested on RT-CES. The comprehensive applications of the RT-CES technique include: real-time monitoring of cell proliferation, inhibition induced by environmental chemical toxicants (Xing, Zhu et al. 2006), natural killer cells (Glamann and Hansen 2006), the siRNA mediated specific gene silencing effect; investigation of different G-protein coupled receptor activity through detection of different patterns of cellular morphological changes (Yu, Atienza et al. 2006); high throughput cell-killing effect screening in the pharmaceutical drug development field (An, Zhu et al. 2006); investigation of diverse attachment interaction between cells and different extra-cellular matrices (Atienza, Zhu et al. 2005) etc. In addition, RT-CES could be used as a unique tool to monitor the quality of live cells in cell-based assays, and thus could be applied to develop other cell-based assays (Kirstein, Atienza et al. 2006).

All together, the RT-CES technique is a sensitive quantitative measurement to evaluate the cellular response to toxicants. The high content and information-rich data it provides could be a suitable tool for rapid high throughput screening and characterizing in vitro cytotoxicity for environmental toxicants.

1.6 Thesis Objectives

The goal of this thesis research is to develop a high throughput toxicity testing techniques and demonstrate their applications to environmental health studies. The

specific objectives include (1) to develop a high throughput cytotoxicity testing method using the RT-CES technique and demonstrate its application to a toxicity study of drinking water disinfection by-products and (2) develop a high throughput toxicity testing method for toxicity screening of air particulates. The major steps of this thesis research are briefly described as the following:

(1) To develop and validate a RT-CES high throughput continuous monitoring assay to study cellular responses resulting from exposure to chemicals.

(2) To demonstrate the application of the new assay in drinking water research. Several N-nitrosamine compounds (N-nitrosodimethylamine (NDMA), N-nitrosopyrrolidine (NPyr), N-nitrosopiperidine (NPip) and N-nitrosodiphenylamine (NDPhA)), which have been recently identified as DBPs in drinking water systems. These compounds are potent animal carcinogens and probable human carcinogens. Thus they will be chosen as the test compounds to demonstrate the application of the RT-CES assay in the evaluation of toxicity of drinking water DBPs. The features of the proposed RT-CES assay will be examined in terms of the dose-dependent, time-dependent, cell-dependent, and compound-dependent cytotoxicity. A panel of four cell lines will be used to test the four N-nitrosamines, and a reversibility assay will also be conducted to obtain more information about their cytotoxcity profile.

(3) To further explain the effects of cytotoxicity detected by the RT-CES assay, we will investigate the mechanisms underlying the cytotoxicites of different compounds. We

will examine whether the cytotoxic effects are due to cell killing or to the inhibition of cell proliferation. We will use the trypan blue stain assay to count the percentage of the dead cells in the total cells, and we will use flow cytometry to perform cell cycle analysis in order to evaluate the anti-proliferation effects.

(4) To develop a novel RT-CES method for testing cytotoxicity of particulate matter. We will initially use quartz particles as model particulate matter and apply the RT-CES method to detect the cytotoxicity of quartz particles.

(5) To demonstrate the application of the new assay to test typical urban air particulates, we will use standard reference materials SRM 1649a (urban dust standard reference material) and SRM 2975 (diesel particle standard reference material) as examples.

(6) To study different mechanisms underlying the cytotoxic effects induced by quartz particles, we will choose two different pulmonary epithelial cell lines, A549 cells (human type II-like cells), and SK-MES-1 cells (human type I-like cells). These cells will be exposed to quartz particles of respirable size, and the cell death modes in response to quartz exposure will be examined. Cell cycle analysis, caspase inhibitor study, MMP assay, and morphological studies will be performed to achieve this goal.

1.7 References

An, H., J. Zhu, et al. (2006). "Synthesis and anti-tumor evaluation of new trisulfide derivatives." *Bioorg Med Chem Lett* **16**(18): 4826-9.

Annesi-Maesano, I. and W. Dab (2006). "[Air pollution and the lung: epidemiological approach]." *Med Sci (Paris)* **22**(6-7): 589-94.

Antony, A. B., R. S. Tepper, et al. (2002). "Cockroach extract antigen increases bronchial airway epithelial permeability." *J Allergy Clin Immunol* **110**(4): 589-95.

Arends, M. J. and A. H. Wyllie (1991). "Apoptosis: mechanisms and roles in pathology." *Int Rev Exp Pathol* **32**: 223-54.

Atienza, J. M., J. Zhu, et al. (2005). "Dynamic monitoring of cell adhesion and spreading on microelectronic sensor arrays." *J Biomol Screen* **10**(8): 795-805.

Baserga, R. (1965). "The Relationship of the Cell Cycle to Tumor Growth and Control of Cell Division: a Review." *Cancer Res* **25**: 581-95.

Boorman, G. A. (1999). "Drinking water disinfection byproducts: review and approach to toxicity evaluation." *Environ Health Perspect* **107 Suppl 1**: 207-17.

Brady, J. F., F. Xiao, et al. (1991). "Effects of disulfiram on hepatic P450IIE1, other microsomal enzymes, and hepatotoxicity in rats." *Toxicol Appl Pharmacol* **108**(2): 366-73.

Bratton, S. B., G. Walker, et al. (2001). "Recruitment, activation and retention of caspases-9 and -3 by Apaf-1 apoptosome and associated XIAP complexes." *Embo J* **20**(5): 998-1009.

Brook, R. D. (2005). "You are what you breathe: evidence linking air pollution and blood pressure." *Curr Hypertens Rep* **7**(6): 427-34.

Brunekreef, B. and B. Forsberg (2005). "Epidemiological evidence of effects of coarse airborne particles on health." *Eur Respir J* **26**(2): 309-18.

Byfield, J. E., I. Weintraub, et al. (1973). "Inhibition of colony formation by cytotoxic antibodies in cervical epidermoid carcinoma." *Radiology* **107**(3): 685-6.

Cain, K., D. G. Brown, et al. (1999). "Caspase activation involves the formation of the aposome, a large (approximately 700 kDa) caspase-activating complex." *J Biol Chem* **274**(32): 22686-92.

Cantor, K. P. (1997). "Drinking water and cancer." Cancer Causes Control **8**(3): 292-308.

Cantor, K. P., C. F. Lynch, et al. (1998). "Drinking water source and chlorination byproducts. I. Risk of bladder cancer." *Epidemiology* **9**(1): 21-8.

Cook, J. A. and J. B. Mitchell (1989). "Viability measurements in mammalian cell systems." *Anal Biochem* **179**(1): 1-7.

Decker, T. and M. L. Lohmann-Matthes (1988). "A quick and simple method for the quantitation of lactate dehydrogenase release in measurements of cellular cytotoxicity and tumor necrosis factor (TNF) activity." *J Immunol Methods* **115**(1): 61-9.

DePaola, N., J. E. Phelps, et al. (2001). "Electrical impedance of cultured endothelium under fluid flow." *Ann Biomed Eng* **29**(8): 648-56.

Diaz, T. M., R. Manez, et al. (2003). "Monitoring cytotoxicity against pig cells after transplantation using two-color fluorescence viability assay." *Transplant Proc* **35**(5): 2047-8.

Fadeel, B., S. Orrenius, et al. (1999). "Apoptosis in human disease: a new skin for the old ceremony?" *Biochem Biophys Res Commun* **266**(3): 699-717.

Fong, R. and F. Kissmeyer-Nielsen (1972). "A combined dye exclusion (trypan blue) and fluorochromatic technique for the microdroplet lymphocytotoxicity test." *Tissue Antigens* **2**(1): 57-63.

Formigli, L., A. Conti, et al. (2004). ""Falling leaves": a survey of the history of apoptosis." *Minerva Med* **95**(2): 159-64.

French, A. S., C. B. Copeland, et al. (1999). "Evaluation of the potential immunotoxicity of bromodichloromethane in rats and mice." *J Toxicol Environ Health A* **56**(5): 297-310.
French, A. S., C. B. Copeland, et al. (1998). "Evaluation of the potential immunotoxicity

of chlorinated drinking water in mice." *Toxicology* **125**(1): 53-8.

Gailit, J. and R. A. Clark (1996). "Studies in vitro on the role of alpha v and beta 1 integrins in the adhesion of human dermal fibroblasts to provisional matrix proteins fibronectin, vitronectin, and fibrinogen." *J Invest Dermatol* **106**(1): 102-8.

Gallagher, M. D., J. R. Nuckols, et al. (1998). "Exposure to trihalomethanes and adverse pregnancy outcomes." *Epidemiology* **9**(5): 484-9.

Gao, X., Q. Yu, et al. (2005). "Health effects of airborne particulate matter trace elements." *Biomed Environ Sci* **18**(5): 349-55.

Giaever, I. and C. R. Keese (1984). "Monitoring fibroblast behavior in tissue culture with an applied electric field." *Proc Natl Acad Sci U S A* **81**(12): 3761-4.

Gillissen, A., C. Gessner, et al. (2006). "[Health significance of inhaled particles]." *Dtsch Med Wochenschr* **131**(12): 639-44.

Glamann, J. and A. J. Hansen (2006). "Dynamic detection of natural killer cell-mediated cytotoxicity and cell adhesion by electrical impedance measurements." *Assay Drug Dev Technol* **4**(5): 555-63.

Glinianaia, S. V., J. Rankin, et al. (2004). "Particulate air pollution and fetal health: a systematic review of the epidemiologic evidence." *Epidemiology* **15**(1): 36-45.

Guo, T. L., J. A. McCay, et al. (2001). "Immunotoxicity of sodium bromate in female B6C3F1 mice: a 28-day drinking water study." *Drug Chem Toxicol* **24**(2): 129-49.

Heinrich, J. and H. E. Wichmann (2004). "Traffic related pollutants in Europe and their effect on allergic disease." *Curr Opin Allergy Clin Immunol* **4**(5): 341-8.

Hsiao, W. L., Z. Y. Mo, et al. (2000). "Cytotoxicity of PM(2.5) and PM(2.5--10) ambient air pollutants assessed by the MTT and the Comet assays." *Mutat Res* **471**(1-2): 45-55.

Huang, N. and D. Xu (2004). "[Advances on the immunotoxicity of airborne fine particulate matter (PM2.5)]." *Wei Sheng Yan Jiu* **33**(3): 365-8.

Igney, F. H. and P. H. Krammer (2002). "Death and anti-death: tumour resistance to apoptosis." *Nat Rev Cancer* **2**(4): 277-88.

John A. Cook, J. B. M. (1989). "Viability Measurements in Mammalian Cell Systems." *Analytical Biochemistry* **179**: 1-7.

Karrow, N. A., T. L. Guo, et al. (2001). "Evaluation of the immunomodulatory effects of the disinfection by-product, sodium chlorite, in female B6C3F1 mice: a drinking water study." *Drug Chem Toxicol* **24**(3): 239-58.

Kerr, J. F., A. H. Wyllie, et al. (1972). "Apoptosis: a basic biological phenomenon with wide-ranging implications in tissue kinetics." *Br J Cancer* **26**(4): 239-57.

Kirstein, S. L., J. M. Atienza, et al. (2006). "Live cell quality control and utility of real-time cell electronic sensing for assay development." *Assay Drug Dev Technol* **4**(5): 545-53.

Kramer, M. D., C. F. Lynch, et al. (1992). "The association of waterborne chloroform with intrauterine growth retardation." *Epidemiology* **3**(5): 407-13.

Lecoeur, H., M. C. Prevost, et al. (2001). "Oncosis is associated with exposure of phosphatidylserine residues on the outside layer of the plasma membrane: a reconsideration of the specificity of the annexin V/propidium iodide assay." *Cytometry* **44**(1): 65-72.

Linder, R. E., G. R. Klinefelter, et al. (1995). "Dibromoacetic acid affects reproductive competence and sperm quality in the male rat." *Fundam Appl Toxicol* **28**(1): 9-17.

Luch, A. (2002). "Cell cycle control and cell division: implications for chemically induced carcinogenesis." *Chembiochem* **3**(6): 506-16.

Lynberg, M., J. R. Nuckols, et al. (2001). "Assessing exposure to disinfection by-products in women of reproductive age living in Corpus Christi, Texas, and Cobb county, Georgia: descriptive results and methods." *Environ Health Perspect* **109**(6): 597-604.

Mather, G. G., J. H. Exon, et al. (1990). "Subchronic 90 day toxicity of dichloroacetic and trichloroacetic acid in rats." *Toxicology* **64**(1): 71-80.

McDorman, K. S., B. F. Pachkowski, et al. (2005). "Oxidative DNA damage from potassium bromate exposure in Long-Evans rats is not enhanced by a mixture of drinking water disinfection by-products." *Chem Biol Interact* **152**(2-3): 107-17.

Moser, V. C., P. M. Phillips, et al. (1999). "Behavioral evaluation of the neurotoxicity produced by dichloroacetic acid in rats." *Neurotoxicol Teratol* **21**(6): 719-31.

Muller, A., G. Wichmann, et al. (2006). "Cytotoxicity and oxidative stress caused by chemicals adsorbed on particulate matter." *Environ Toxicol* **21**(5): 457-463.

Musafia-Jeknic, T., B. Mahadevan, et al. (2005). "Long-term effects of a standardized complex mixture of urban dust particulate on the metabolic activation of carcinogenic polycyclic aromatic hydrocarbons in human cells in culture." *Toxicol Sci* **88**(2): 358-66.

Muzio, M., A. M. Chinnaiyan, et al. (1996). "FLICE, a novel FADD-homologous ICE/CED-3-like protease, is recruited to the CD95 (Fas/APO-1) death--inducing signaling complex." *Cell* **85**(6): 817-27.

Nuckols, J. R., D. L. Ashley, et al. (2005). "Influence of tap water quality and household water use activities on indoor air and internal dose levels of trihalomethanes." *Environ Health Perspect* **113**(7): 863-70.

Ramirez-Icaza, G., K. A. Mohammed, et al. (2004). "Th2 cytokines IL-4 and IL-13 downregulate paxillin expression in bronchial airway epithelial cells." *J Clin Immunol* **24**(4): 426-34.

Richardson, S. D., J. E. Simmons, et al. (2002). "Disinfection byproducts: The next generation." *Environmental Science & Technology* **36**(9): http://pubs.acs.org.login.ezproxy.library.ualberta.ca/cgi-bin/article.cgi/esthag-a/0000/36/i09/html/09rich.html198A-205A.

Saleh, A., S. M. Srinivasula, et al. (1999). "Cytochrome c and dATP-mediated oligomerization of Apaf-1 is a prerequisite for procaspase-9 activation." *J Biol Chem* **274**(25): 17941-5.

Sharma, K. V., C. Koenigsberger, et al. (2001). "Direct evidence for an adhesive function in the noncholinergic role of acetylcholinesterase in neurite outgrowth." *J Neurosci Res* **63**(2): 165-75.

Simmons, J. E., L. K. Teuschler, et al. (2004). "Component-based and whole-mixture techniques for addressing the toxicity of drinking-water disinfection by-product mixtures." *J Toxicol Environ Health A* **67**(8-10): 741-54.

Solly, K., X. Wang, et al. (2004). "Application of real-time cell electronic sensing (RT-CES) technology to cell-based assays." *Assay Drug Dev Technol* **2**(4): 363-72.

Stratford, I. J. and M. A. Stephens (1989). "The differential hypoxic cytotoxicity of bioreductive agents determined in vitro by the MTT assay." *Int J Radiat Oncol Biol Phys* **16**(4): 973-6.

Swan, S. H., K. Waller, et al. (1998). "A prospective study of spontaneous abortion: relation to amount and source of drinking water consumed in early pregnancy." *Epidemiology* **9**(2): 126-33.

Takahashi, A. and W. C. Earnshaw (1996). "ICE-related proteases in apoptosis." *Curr Opin Genet Dev* **6**(1): 50-5.

Wainwright, L. J., A. Lasorella, et al. (2001). "Distinct mechanisms of cell cycle arrest control the decision between differentiation and senescence in human neuroblastoma cells." *Proc Natl Acad Sci U S A* **98**(16): 9396-400.

Walczak, H. and P. H. Krammer (2000). "The CD95 (APO-1/Fas) and the TRAIL (APO-2L) apoptosis systems." *Exp Cell Res* **256**(1): 58-66.

Walczak, H. and M. R. Sprick (2001). "Biochemistry and function of the DISC." *Trends Biochem Sci* **26**(7): 452-3.

Waller, K., S. H. Swan, et al. (1998). "Trihalomethanes in drinking water and spontaneous abortion." *Epidemiology* **9**(2): 134-40.

Xing, J. Z., L. Zhu, et al. (2006). "Microelectronic cell sensor assay for detection of cytotoxicity and prediction of acute toxicity." *Toxicol In Vitro* 20(6): 995-1004.

Xing, J. Z., L. Zhu, et al. (2005). "Dynamic monitoring of cytotoxicity on microelectronic sensors." *Chem Res Toxicol* **18**(2): 154-61.

Zou, H., Y. Li, et al. (1999). "An APAF-1.cytochrome c multimeric complex is a functional apoptosome that activates procaspase-9." *J Biol Chem* **274**(17): 11549-56.

Chapter 2: Development of a Cell-Microelectronic Sensing Technique for the Detection of Cytotoxicity of Newly Discovered Disinfection By-Products and Consequent Mechanistic Study

2.1 Introduction

The occurrence of N-nitrosamines in source water, wastewater, and finished drinking water is an emerging issue of environmental and public health significance because these compounds are potent carcinogens. N-nitrosodimethylamine (NDMA), a member of the family of N-nitrosamines, was first discovered as a disinfection by-product (DBP) in drinking water in 1989 in Ontario, Canada ((Jobb et al. 1994). Consequently, a survey of 145 Ontario drinking water plants was conducted and it was found that NDMA concentration in treated water from most plants was less than 5 ng/L (MOE, 1998).

In 1999, an extremely high concentration of NDMA was discovered in drinking water wells throughout California near rocket engine testing facilities (DHS, 2002), and this prompted the California Department of Health Services to conduct a similar survey of NDMA concentrations in 32 drinking water systems in 2001. The results showed that three of the 20 chloraminated supplies and one of the four water supplies that used anion

exchange treatment surveyed contained NDMA concentration greater than 10 ng/L, while none of eight water supplies that used only free chlorine disinfection exhibited NDMA levels above 5 ng/L (DHS, 2002).

NDMA in drinking water is formed due to reactions between disinfectants (e.g., chloramine and chlorine) and natural organic nitro-compounds. To date, four probable pathways are proposed for the formation of NDMA during the water disinfection process. (1) NDMA is formed from the reaction of dimethylamine (DMA) and monochloramine (a disinfectant residual). Unsymmetrical dimethylhydrazine (UDMH) serves as the intermediate in this two-step process (Mitch and Sedlak 2002). This pathway was supported by the discovery that a relatively higher concentration of NDMA was detected in utilities using chloramines as the disinfectant compared to those using free chlorine. (2) Precursors in source water or wastewater effluent react with free chlorine in the presence of ammonia to produce NDMA (Choi and Valentine 2002; Mitch, Gerecke et al. 2003). The reaction occurs through the formation of monochloramine by the reaction of chlorine and ammonia; the monochloramine formed subsequently reacts with DMA through same UDMH pathway. Thus NDMA is a problematic concern for utilities applying chlorine disinfection of non-nitrified secondary municipal wastewater effluents (Choi and Valentine 2002). (3) NDMA can also be formed in the absence of ammonia through the reaction of hypochlorite with secondary amines. The rate of this reaction is an order of magnitude lower than that observed with monochloramine (Mitch and Sedlak 2002). (4)

A recent study demonstrated the important roles of dichloramine and dissolved oxygen in the formation of NDMA during the disinfection process. The intermediate of this reaction is chlorinated unsymmetrical dialkylhydrazine; the it is further oxygenized by dissolved oxygen to form nitrosamines. The rate of this reaction is three orders of magnitude faster than the reaction of DMA and monochloramine (Schreiber and Mitch 2006). This improved understanding of the nitrosamine formation pathways will facilitate the development of strategic means to reduce its formation during various disinfection processes.

NDMA formation is more prominent in utilities using disinfected wastewater as a recharging source of aquifer because in wastewater much more dissolved organic nitrogen (DON) precursors are relatively persistent than in normal water (Mitch and Sedlak 2004). In addition, the high concentration of ammonia in wastewater will facilitate the formation of NDMA (Schreiber and Mitch 2006).

In spite of the high carcinogenicity of NDMA and its high occurrence as a DBP in drinking water discoverd by these surveys and studies, currently there are no federal Maximum Contaminant Levels (MCLs) for NDMA in drinking water either in Canada or the U.S. The Ontario Ministry of the Environment and Energy established an Interim Maximum Acceptable Concentration (IMAC) of 9 ng/L for NDMA (MOE, 2006) and the California Department of Health Services set an interim action level of 10 ng/L, (DHS, 2006).

Recently, in parallel with more sensitive analytical methods becoming available, more N-nitrosamines were identified as DBPs in drinking water distribution systems. Our laboratory has recently identified several N-nitrosamine compounds in drinking water, including NPyr, NPip, and NDPhA (Charrois, Arend et al. 2004; Zhao, Boyd et al. 2006). Those discoveries and the existing knowledge of the carcinogenicity of N-nitrosamines attract more interest to formation, exposure assessment, and toxicity study of nitrosamines as a family of potential highly toxic unregulated DBPs.

The toxicity of N-nitrosamines had been studied for several decades since the 1960s when nitrosamines were found to exist ubiquitously in food and consumer products, such as beer, meats cured with nitrate, tobacco smoke, and rubber products (Shvemberger 1967). Most of these studies focused on the investigation of the potential carcinogenicity of nitrosamines (IARC, 1978). Based on the results of those studies, the US EPA Integrated Risk Information System (IRIS) has classified NDMA, NPip, and NPyr as probable human carcinogens. The lifetime risk levels estimated at 1 in a million (1×10^{-6}) for NDMA, NPip, and NPyr, are 0.7 ng/L, 3.5 ng/L, and 15 ng/L of drinking water, respectively. NDPhA was classified as a possible human carcinogen.

Besides carcinogenicity and genotoxicity, the hepatotoxicity of NDMA has been noted and studied widely both in vivo and in vitro. However, other toxicity information of NPyr, NPip, NDPhA other than genotoxicity is considerably scarce. Limited or no toxicity information makes their potential inclusion in a contaminants monitoring list

more difficult. This is also a concern for utilities that switch their water treatment to other disinfection methods to reduce the concentration of regulated DBPs; this, however, may promote the formation of more toxic, unregulated and unmonitored DBPs, including N-nitrosamines. Currently, there are more than 500 DBPs with limited toxicity information identified in drinking water systems (Richardson, Simmons et al. 2002). Ranking the unregulated emerging DBPs and comparing their cytotoxicity and genotoxicity to those of regulated DBPs is an effective way to screen and prioritize research efforts. Because of the ethical issues and high cost of in vivo animal toxicity experiments, a method is required to rapidly screen the cytotoxicity of new emerging DBPs to provide toxicity comparisons under uniform experimental conditions.

The conventional cell-based assays usually apply labeling materials or dyes to label and detect the cell viability at one given time-point, and thus can not provide dynamic information on the entire cellular dynamic biological process in response to toxicant exposure. To address this problem, the RT-CES technique has been developed as a suitable breakthrough technique to monitor cytotoxic responses in a real-time, continuous manner. The basic principle and components of RT-CES system have been discussed in Chapter 1.

The objectives of the present study are to: (1) establish the RT-CES method for dynamic detection of the cytotoxicity of environmental chemical contaminants; (2) apply this technique to examine the cell-dependent, time-dependent, and compound-dependent

cytotoxicity of four nitrosamines on four mammalian cells; (3) investigate different underlying mechanisms of different cytotoxicities.

Table 2-1 summarizes the molecular formula, structures, and molecular weight of the four nitrosamines included in this study.

Table 2-1. N-Nitrosamine Species Investigated.

compound	abbreviation	molecular formula	molecular structure	molecular weight
N-nitrosodimethylamine	NDMA	$C_2H_6N_2O$	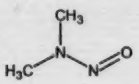	74
N-nitrosopyrrolidine	NPyr	$C_4H_8N_2O$	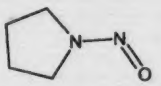	100
N-nitrosopiperidine	NPip	$C_5H_{10}N_2O$	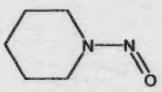	114
N-nitrosodiphenylamine	NDPhA	$C_{12}H_{10}N_2O$	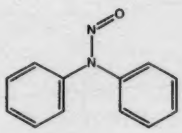	198

2.2 Materials and Methods

2.2.1 Chemicals and Media

NDMA, NPip, NPyr, and NDPhA were purchased from Sigma-Aldrich. (Milwaukee, WI). Pure methanol and reagent water were obtained from Fisher Scientific (Nepean, ON). Cell culture medium, RMPI 1640 for A549 cells was obtained from Sigma Aldrich; McCoy's 5A modified medium for T24 cells was supplied by ATCC; and Dulbecco's Modified Eagle Medium (DMEM)/Ham's F12 for CHO-K1 and DMEM for Hep G2 cells were obtained from Gibco (Los Angeles, USA). Fetal bovine serum was purchased from Sigma Aldrich, and penicillin/streptomycin was obtained from Gibco Co.

2.2.2 Cell Culture and Growth Conditions

Four cell lines, A549, T24, CHO-K1, and Hep G_2 were purchased from the American Type Culture Collection (ATCC, Manassas, VA). These cell lines were cultured using specific media: A549 in RMPI 1640 medium, T24 in McCoy's 5A modified medium, CHO-K1 in Dulbecco's Modified Eagle Medium (DMEM)/Ham's F12, and Hep G_2 in DMEM. Each culture was supplemented with 10% fetal bovine serum and 1% penicillin/streptomycin. The cell cultures were maintained at 37 °C in a 5% CO_2 incubator. The cells grew on a 10 cm Petri dishes and were subcultured every 3–5 days depending on the growth rate and seeding density.

2.2.3 Calibration of Real-Time Cell Electronic Sensing System

The configuration and principle of RT-CES system were described in Chapter 1. To demonstrate the correlation between the cell index and the quantity of cell and to obtain the most suitable starting number of each cell line, calibration studies were conducted for each. The calibration procedure involves three steps: background check of E-plates (step 1), seeding the cells (step 2), and detection of cell index (step 3).

Step 1: 50 μL fresh medium was addressed into each well on the E-plate, and kept at room temperature for 30 min before the E-plate were connected to the sensor station located in the CO2 incubator. The background check of each well was performed under the control of the RT-CES software. The wells with strong background imply problems with signal collection and thus could not be used for further work.

Step 2: After the background check, we addressed different numbers of cells (2500, 5000, 10000, and 20000) in 100 μL medium to individual wells (with good background) on the E-plates. The E-plates seeded with cells were covered and kept at room temperature for 30 min to allow the cells to precipitate and attach to the microelectrodes before connecting the E-plates to the sensor station.

Step 3: Under the control of the RT-CES software, the cell index was monitored for 72 h and automatically recorded with a data collecting rate of once each hour for 72 hr. Calibration curves based on the cell index (CI) versus the number of cells seeded for each test cell line were obtained and linear analysis were conducted to determine the optimized starting number of cells.

2.2.4 Detection of Cytotoxicity of Four Nitrosamines in Four Different Cells

The procedure of the cytotoxicity test involves four steps: background check of the E-plates (step 1), seeding the cells (step 2), delivering compounds to be tested (step 3) and detection of cell index (step 4).

Step 1: Background check (same as step 1 in the calibration part of the system).

Step 2: After the background check, we created a map corresponding to each E-plate, marking the starting cell number, cell line name, and compound name and concentration for each available well. According to the map, a population of cells in 100 μL was seeded to each individual well on the E-plates following the same procedure as in step 2 of the calibration.

Step 3: RT-CES automatically monitored the cell index of each well. As the cell growth reached the exponential phase (the cell index increased to around 1), we took the E-plate out of the incubator, and replaced the medium in each well with medium containing nitrosamines. NDMA, NPyr, and NPip were dissolved in fresh media whereas NDPhA was dissolved in ethanol at a proportion of 1% per 5 mM of NDPhA and was diluted to desired concentration. After the addition of nitrosamines, the E-plates were reconnected to the sensor station.

Step 4: the change in the cell index of each well was recorded automatically every hour for another 60–70 hr. The data was further processed to get the EC_{50} by using prism software.

2.2.5 Reversibility Study

To examine whether the effects of nitrosamines on different cells are reversible, we carried out the reversibility study by using the RT-CES method. The cells were first exposed to nitrosamines for 24 h before the medium containing compounds was removed and exchanged with fresh chemical-free medium. Another set of control experiments was performed in parallel, in which the cells were exposed to the nitrosamines at the same concentrations without the replacement of fresh chemical-free medium. The cell indexes obtained from the cells with and without the replacement of fresh medium were compared to evaluate the reversibility.

2.2.6 Trypan Blue Stain Assay

To differentiate the effects of nitrosamines as killing the cells or as inhibiting the growth of the cells, we used the trypan blue staining assay to differentiate between live and dead cells. Trypan blue is a negatively charged vital dye, and thus it can not enter live cells. When the cells are dead and their membranes are damaged, this dye can enter the cells and react with DNA to show a dark blue color. The dead cells are stained dark blue and the live cells are not stained, thus differentiating dead cells from live ones.

The procedures for Trypan blue staining: after the cells were treated with four N-nitrosamine compounds for 24 h, they were harvested and diluted at certain times according to cell density with phosphate-buffered saline buffer (pH 7.2) (Gibco) and mixed well. Cell suspensions of 20 μL each were mixed with 50 μL Trypan blue and 30 μL PBS and stained for 5 min. The number of dead cells and total cells was counted using a hemocytometer (Fisher Scientific) and the percentage of dead cells in the total cells was calculated.

2.2.7 Cell Cycle Analysis

Distribution of cells among the cell cycle stages after nitrosamine treatment was analyzed using flow cytometry according to a previously described method (Nicoletti, Migliorati et al. 1991). Cells were collected and centrifuged (300 g for 3 min), washed with ice-cold PBS, centrifuged again, then fixed in 70% ethanol overnight at 4 °C. Cells were resuspended in PBS (Gibco) containing 0.1% Triton X-100 (VWR International, Mississauga, ON), 100 µg/mL RNase A (Sigma Aldrich), and 330 µg/mL propidium iodide (Sigma Aldrich) and incubated for 30 min at 37 °C in a dark room. Cell cycle analysis was performed using a Becton and Dickinson FACScanTM (Montain View, CA). Data analysis was performed using Cell QuestTM software (Becton and Dickinson).

2.3 Results and Discussion

2.3.1 The Selection of Four In Vitro Models for Detecting the Cytotoxicity of DBPs

A label-free, real-time RT-CES technique was developed to measure the different cytotoxicity of four nitrosamines on four mammalian cell lines. Three human cell lines (A549, T24, HepG2, derived from lung, bladder, and liver carcinoma cells) and Chinese Hamster Ovary (CHO-K1) cells were chosen for this study, based on the following rationale: (1) CHO-K1 cells are normal mammalian cells which have been used in several recent DBP cytotoxicity and genotoxicity studies (Plewa, Kargalioglu et al. 2002; Plewa, Wagner et al. 2004); (2) Individual exposure to DBPs in drinking water could occur through ingestion, inhalation, and dermal exposure. The blood and exhaled air concentrations of volatile DBPs are much higher when exposed results from showering or

bathing than from drinking tap water (Backer, Ashley et al. 2000). The aerosols generated during showering or bathing with hot water could be inhaled and thus could enter into the bloodstream directly, escaping from the first pass effect. Nitrosamines are volatile DBPs, thus exposure through showering and bathing is reasonably expected to be of importance. The lungs are vital organs that encounter aerosols when exposed to them in the inhaled air, so we included lung epithelial cells in our study. (3) Bladder cancer has been associated with disinfected drinking water consumption, strongly supported by many epidemiological studies. (4) NDMA has also been reported to be a potent hepatotoxicant in mice and rats through CYP2E1 activation (Brady, Xiao et al. 1991). HepG2 cells are a commonly used in vitro model to test hepatotoxicity.

2.3.2 Calibration Results of RT-CES for Four Cells

The calibration of each cell line was required before the cytotoxicity assay to validate the method and obtain the most suitable starting number for each cell line. Different numbers of cells (2500, 5000, 10000, and 20000) were seeded on to the E-plates, and the change in the cell index of each well was monitored continuously for 72 h. The linear regression analysis was further conducted using Excel software (Microsoft, Redmond, WA).

The results are shown in Figure 2-1. Graphs A-D show cell growth curves recorded by the RT-CES system; each curve represents the average cell index of six replicate wells seeded with cells at a specific number versus time. The cell index started at 0 and

increased gradually as the cells started to attach and grow on top of the electrodes embedded at the bottom of the wells. After growing for a certain time period, the cells covered all the bottom area of the well and stopped growing due to the cell-cell contact inhibition effect, and thus the cell index reaches a plateau phase from then on. The different cells reach the plateau phase at different times depending on their characteristic growth rate. The linear regression analysis indicates that the cell indexes obtained from the RT-CES system correlate with the starting cell numbers before the cells reached the plateau phase. In addition, the calibration curves help to determine the optimal starting number for each cell line based on the criterion that at this starting number the cells could keep growing for 80 h before the growth curve reaches the plateau phase. The starting numbers for A549, T24, CHO-K1, and HepG2 in the subsequent cytotoxicity testing of the DBPs were chosen to be 3000, 4000, 5000, and 15000, respectively, according to the criterion mentioned above.

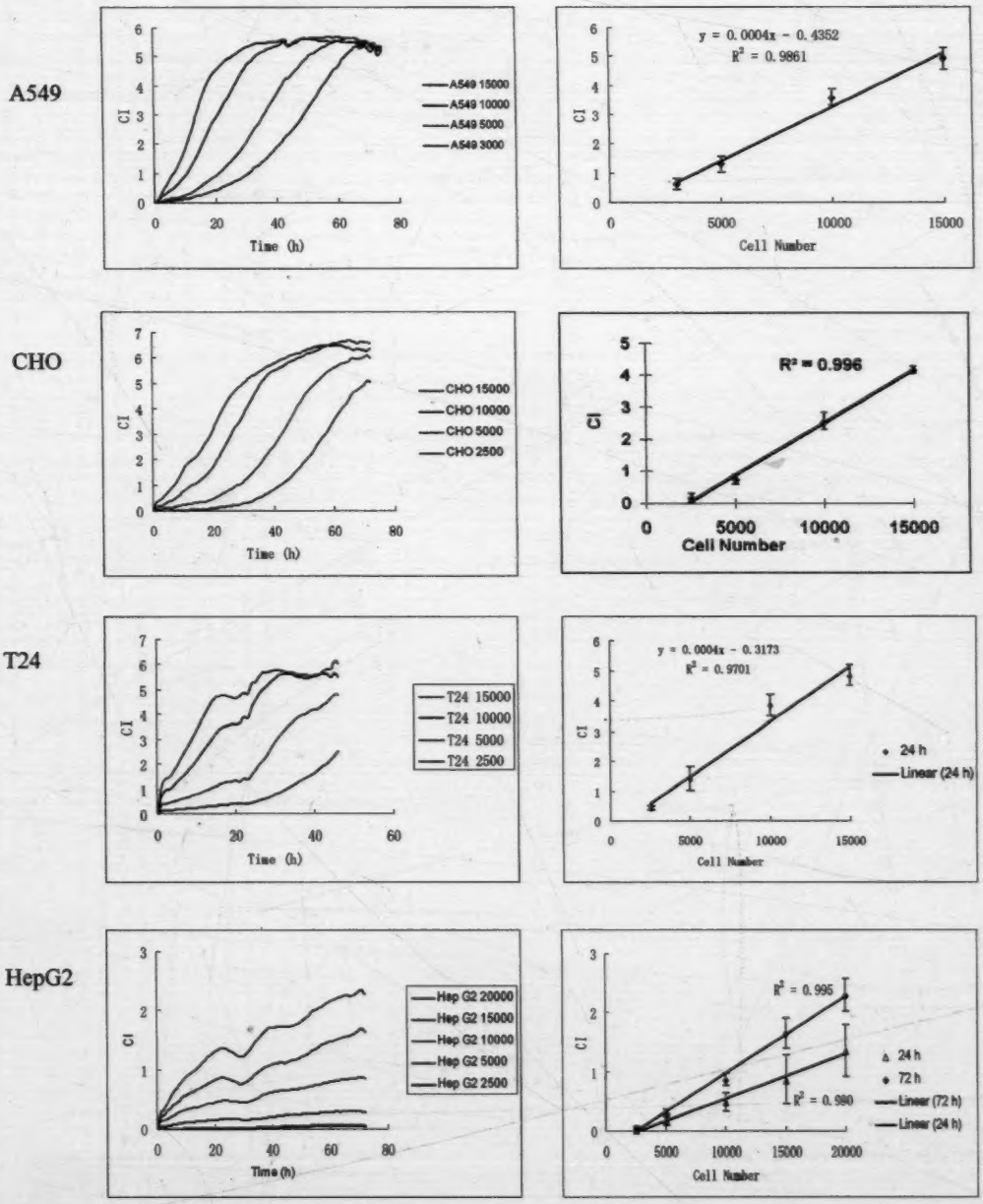

Figure 2-1. Calibration curves of different cell lines and the correlations between the CI at 24 h and 72 h obtained from RT-CES and the cell number.

2.3.3 Cytotoxicity of Nitrosamines Determined by RT-CES Method

The RT-CES technique was applied to continuously measure the real-time cytotoxicity of four nitrosamines on four cell lines. Nitrosamines were added to the cell media at 24 h, and the cells were automatically monitored for another 76 h. RT-CES response curves (cell index versus time) of four cell lines towards nitrosamine treatment and subsequent dose-response analysis are shown in Figures 2-2, 2-3, 2-4, and 2-5. Each curve represents the changes in the average cell index of cells from three wells with the same treatment over time, thus reflecting the biological response of cells towards a certain concentration of a particular nitrosamine. The dose response analysis was conducted using Graphpad Prism Software (San Diego, CA). To conduct the dose response analysis, cell indexes of each well at 24, 36, 48, 60, and 72 h were first transformed to the percentage of the average cell index of the control wells at the same time point. The transformed cell index and dose level were further fitted using a sigmoid non-linear regression model and IC_{50}s were obtained at several time-points. Each chemical has a particular IC_{50} on a particular cell. The IC_{50} represents the concentration of nitrosamine that causes a 50% reduction of CI towards toxicant exposure. The lower the IC_{50}, the more potent the cytotoxicity is.

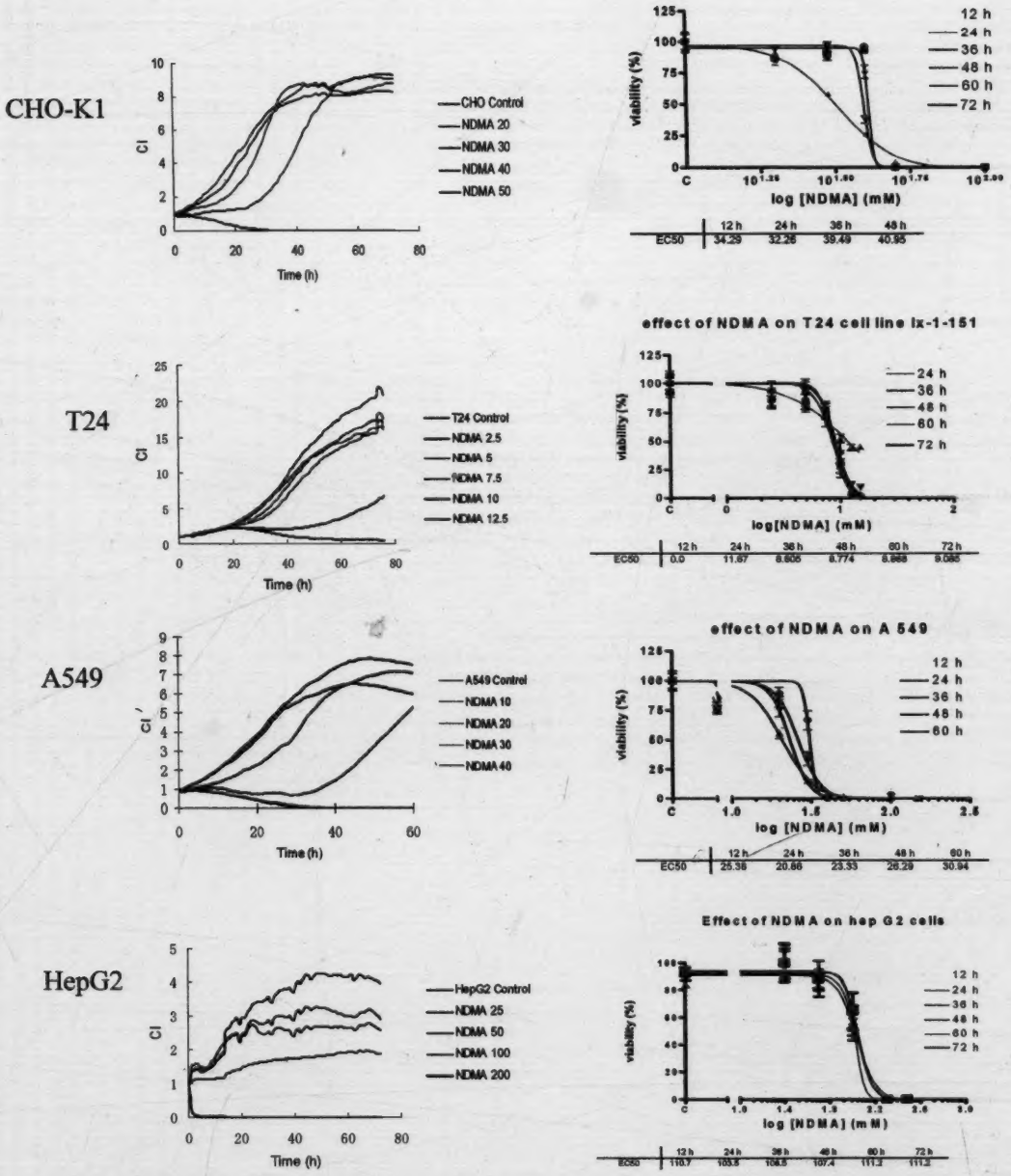

Figure 2-2. The responses of CHO-K1, A549, T24, and $HepG_2$ cells towards NDMA exposure.

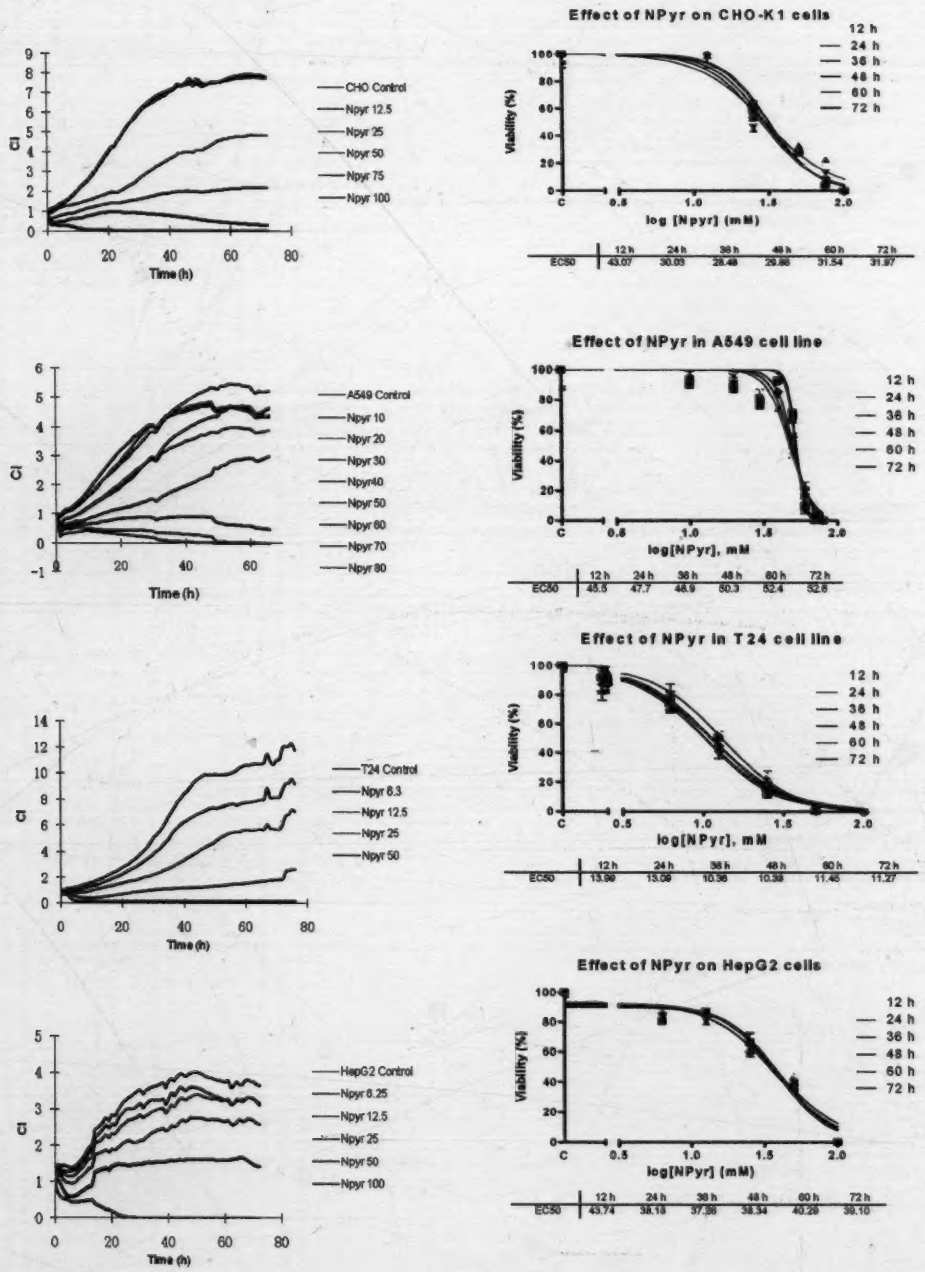

Figure 2-3. The responses of CHO-K1, A549, T24, and $HepG_2$ cells towards NPyr exposure.

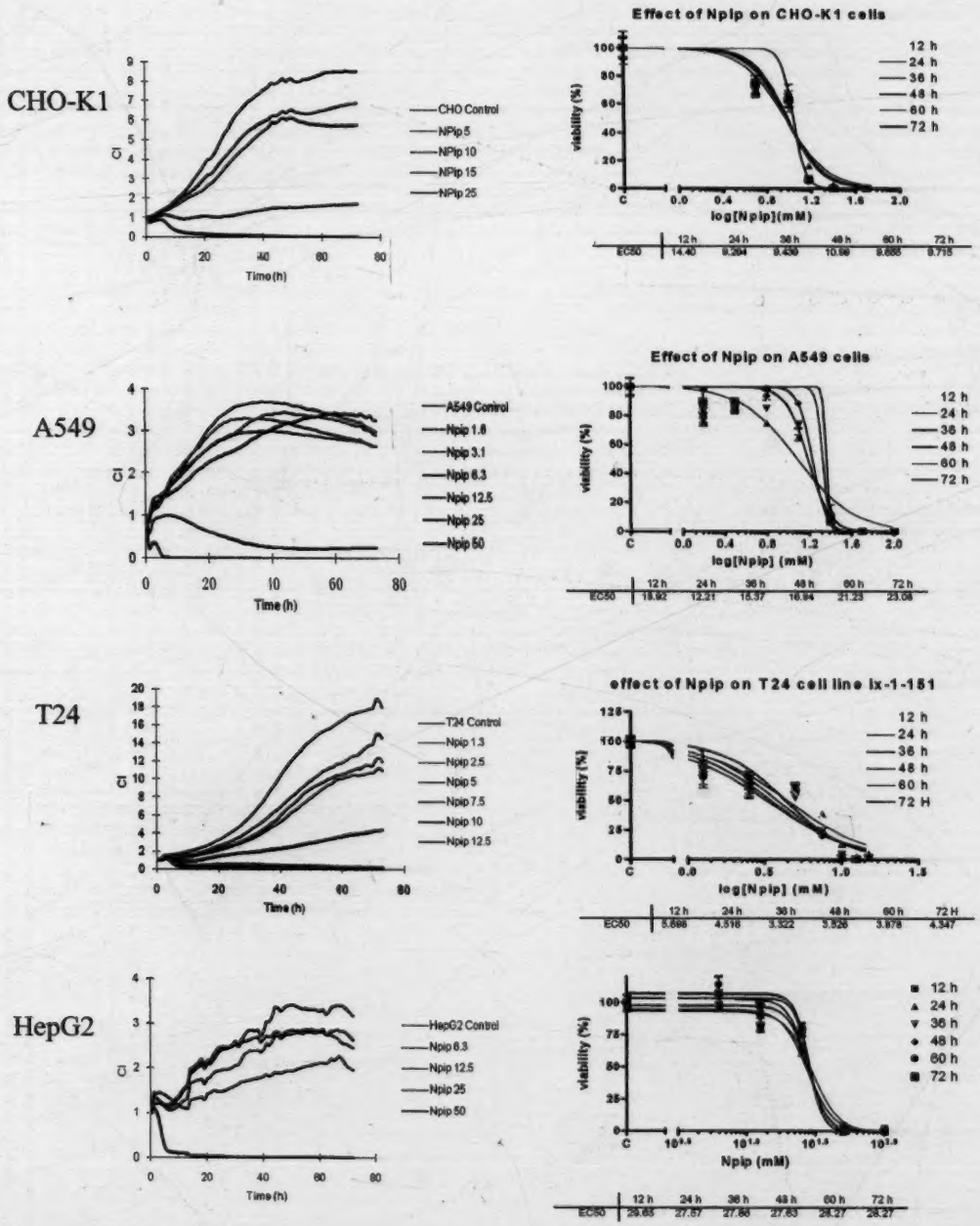

Figure 2-4. The responses of CHO-K1, A549, T24, $HepG_2$ cells towards NPip exposure.

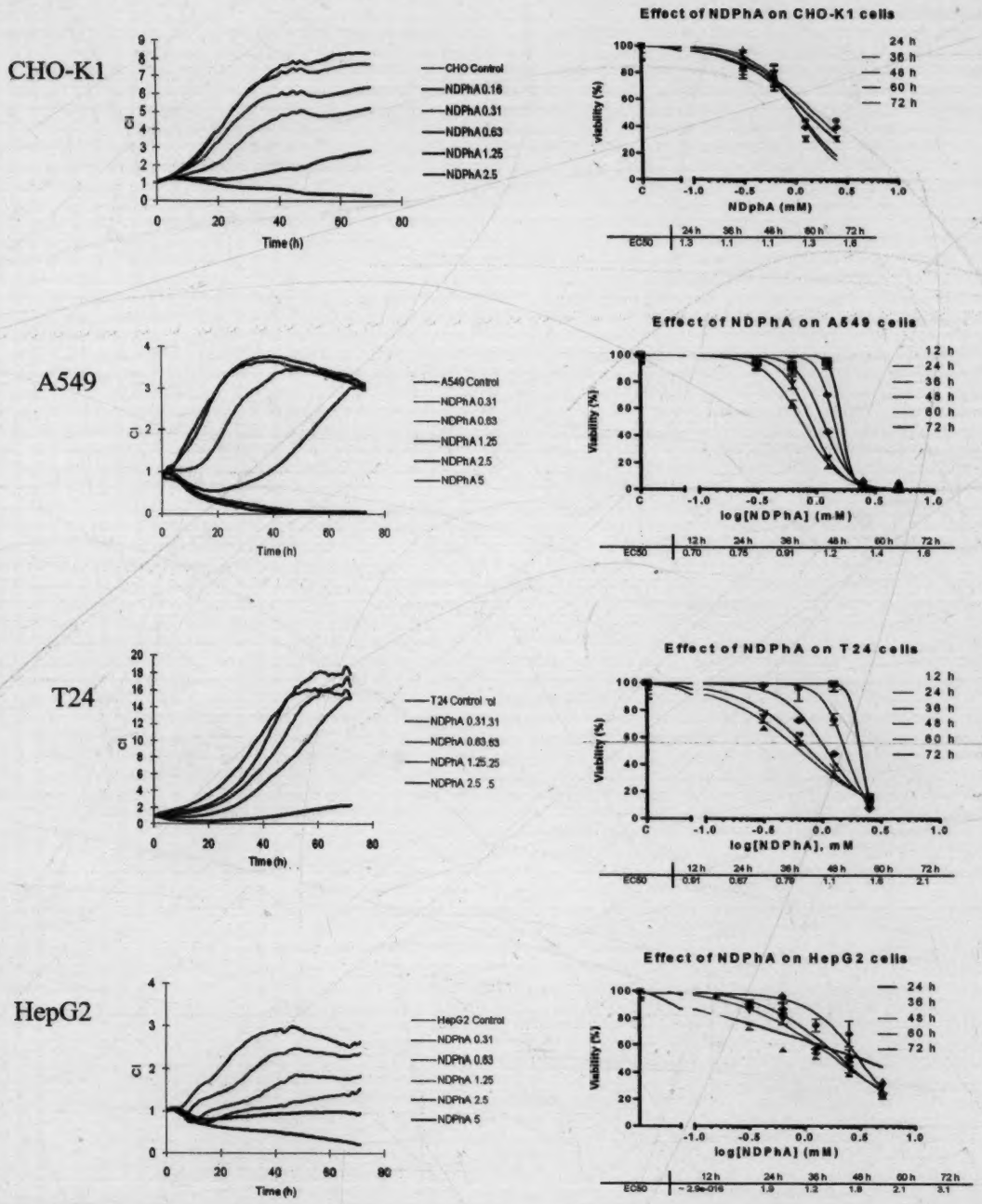

Figure 2-5. The responses of CHO-K1, A549, T24, and $HepG_2$ cells towards NDPhA exposure.

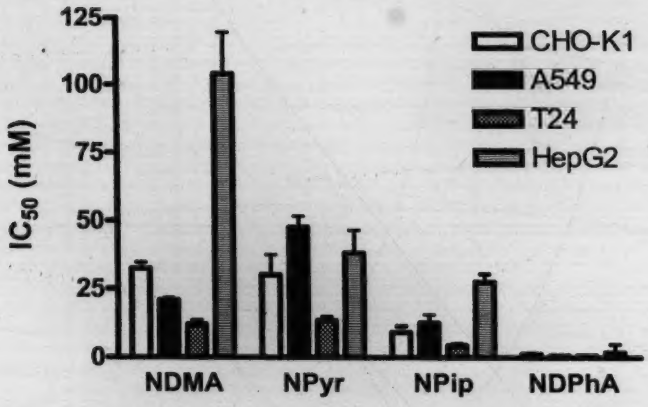

Figure 2-6. Comparison of IC_{50} values at 24 h of four nitrosamines on four cell lines. The IC_{50} values were expressed as the mean value with 95% confidence interval.

Figure 2-6 summarizes the IC_{50} values at 24 h of four compounds on each cell line and demonstrated the dose-dependent, cell-dependent cytotoxicity. There is approximately 154 times difference in the IC_{50} values ranging from a value of 0.67 mM for NDPhA on T24 cells and 103.5 mM for NDMA on Hep G2 cells. The rank order of the four compounds in order of decreasing toxicity is: NDPhA > NPip > NDMA > NPyr on CHO-K1, A549, and T24 cells and NDPhA > NPip > NPyr > NDMA on $HepG_2$. These results indicate that NDPhA is the most cytotoxic among the four nitrosamines tested. The IC_{50} of NDPhA is 30 times lower (1.3 mM) than that of NDMA (32.3 mM) in CHO cells. A few studies revealed that NDPhA is much less potent in terms of genotoxicity and carcinogenicity than the other three nitrosamines (Negishi, Shiotani et al. 1991) whereas the potent cytotoxicity of NDPhA may be neglected.

Table 2-2: Nitrosamine Cytotoxicity Results on Four Cell Lines.

	NDMA				NPyr			
	CHO-K1	A549	T24	HepG2	CHO-K1	A549	T24	HepG2
Minimum Response Dose[a] (mM)	30	20	2.5	25*	13	40	3.2	6.25
Maximum Response Dose[b] (mM)	50	40	13	200	100	70	50	100
$IC_{50(48h)}$[c]	32.3	20.9	11.7	104	30.0	47.7	13.1	38.2
(95% CI)	(30.1-34.6)	(20.1-21.7)	(10.3-13.3)	(44.3-242)	(18.9-47.7)	(43.9-51.7)	(11.7-11.6)	(30.6-47.6)
Minimum $IC_{50(Time)}$[e] (mM)	32.3 (48 h)	20.9 (48 h)	8.6 (60 h)	103.5 (48 h)	28.5 (60 h)	45.5 (36 h)	10.4 (60 h)	38.2 (48 h)
	NPip				NDPhA			
	CHO-K1	A549	T24	HepG2	CHO-K1	A549	T24	HepG2
Minimum Response Dose[a] (mM)	5.0*	13	1.6	3.2	0.31	0.63	0.31	0.31*
Maximum Response Dose[b] (mM)	25	50	10	50	2.5	2.5	2.5	5
$IC_{50(24h)}$[c]	9.3	12.2	4.5	27.6	1.3	0.75	0.67	1.9
(95% CI)	(7.6-11.4)	(9.7-15.4)	(3.8-5.3)	(25.0-30.5)	(0.9-1.9)	(0.7-0.8)	(0.57-0.78)	(0.77-4.9)
Minimum $IC_{50(Time)}$[e] (mM)	9.3 (24 h)	12.2 (24 h)	3.3 (36 h)	27.6 (24 h)	1.1 (36 h)	0.7 (12 h)	0.7 (24 h)	1.2 (36 h)

[a] The highest concentration that generated no cytotoxic response compared to the control. Values reported are based on actual concentrations tested. * indicates lowest concentration tested but some cytotoxic response observed.

[b] The lowest concentration that generated maximum cytotoxic effect at 24 h following nitrosamine addition. Values reported are based on actual concentrations tested.

[c] IC_{50} is the concentration at which a 50% reduction in cell index is observed. $IC_{50(48\ h)}$ was calculated at 48 h after the beginning of the experiment (Nitrosamines were added to the cell media at 24 h).

[d] Lowest IC_{50} observed at the indicated time from the beginning of the experiment (nitrosamines were added to the cell media at 24 h).

Table 2-2 summarizes the cytotoxicity characteristics of nitrosamines on all four cell lines. The maximum response dose is the lowest concentration at which the cell index drops to zero at 24 h after administration of nitrosamine. The minimum response dose is the highest concentration of nitrosamines at which no biological responses could be observed at 24 h. $IC_{50\ (24\ h)}$ indicates the concentration of nitrosamine at which the cell index dropped 50% at 24 h and is expressed by the mean and a 95% confidence interval. The minimum IC_{50} is the lowest IC_{50} at a specific time-point, at which the cytotoxicity is the most potent.

2.3.4 Cell Line Specific Cytotoxicity

The sensitivity of the four mammalian cell lines to each nitrosamine was also investigated. T24 cells were most sensitive of the four cell lines for each nitrosamine tested as determined by the IC_{50}. This suggests that T24 may be an appropriate cell line for sensitive detection of cytotoxic effects of DBPs. HepG2 cells were the least sensitive cell line, even for NDMA, which had been shown to cause potent hepatotoxocity in rats and humans (Valentin-Severin, Le Hegarat et al. 2003). HepG2 cells have been used as a popular in vitro model to test the genotoxicity and hepatotoxicity of nitrosamines in many studies (Uhl, Helma et al. 1999; Uhl, Helma et al. 2000; Valentin-Severin, Le Hegarat et al. 2003). The cytotoxicity of NDMA on HepG2 cells had been tested by measuring the effects on RNA synthesis inhibition; the IC_{50} was reported to be 110 mM (Valentin-Severin, Le Hegarat et al. 2003), which was comparable with our results of

103.5 mM. The responsible reasons for the low sensitivity may be that the expression levels of phase I enzymes are much lower in $HepG_2$ cells than in normal human liver cells. There is evidence that the ratios of mRNA levels between human primary liver cells and $HepG_2$ cells range from 13.71 to 5027.60, and that there is 1460 times more CYP2E1 mRNA in human primary hepatocytes than in HepG2 cells (Brady, Xiao et al. 1991; Anundi and Lindros 1992; Wilkening, Stahl et al. 2003). NPip and NPyr are two structurally similar nitrosamine species, metabolized mainly by CYP2As through α-hydrolation (Wong, Murphy et al. 2005). The fact that the catalytic activities of CYP2A1 in HepG2 are ten times higher than CYP2E1 (Grogan, Shou et al. 1995) partially explained why HepG2 cells are more sensitive to NPyr and NPip exposure than to NDMA. Though primary hepatocytes have the advantages, similar morphological and physiological characteristics as human normal liver cells, the shortage of human liver material, the lack of ability to proliferate, and the loss of metabolizing ability within weeks limit their application as preferred research tools (Wilkening, Stahl et al. 2003). Searching for other robust human liver cell lines may be appropriate for the toxicity testing of chemicals that are metabolized by P450 enzymes. The rank order of cell sensitivity from most to least to nitrosamines is: T24 > A549 > CHO > HepG2.

2.3.5 Reversibility Study

Another characteristic of cytotoxicity is reversibility, which measures the ability of cells to recover from cytotoxic damage. To perform the reversibility study, CHO-K1 cells

and A549 cells were first exposed to different dose levels of nitrosamines for 24 h, after which the media containing nitrosamines were replaced by fresh chemical-free media, and the cell index changes were continuously observed for another 48 h, another set of experiments was conducted in parallel under same condition but without replacement of nitrosamine-laden media. Figure 2-8 shows the reversibility studies. The cytotoxic effects of NDMA are the least reversible, demonstrated by the small recovery observed in one concentration (50 mM) in CHO-K1 cells only. For NPip and NPyr, the cells recovered rapidly after replacement of the medium, which means that the impact of NPyr and NPip on the cells is not permanent and that cells could recover completely after removal of exposure. The cytotoxic effect of NDPhA was more reversible compared with that of NDMA, but not as prominent as that of NPyr and NPip. The rank order of reversibility of four nitrosamines is: NPyr > NPip > NDPhA > NDMA.

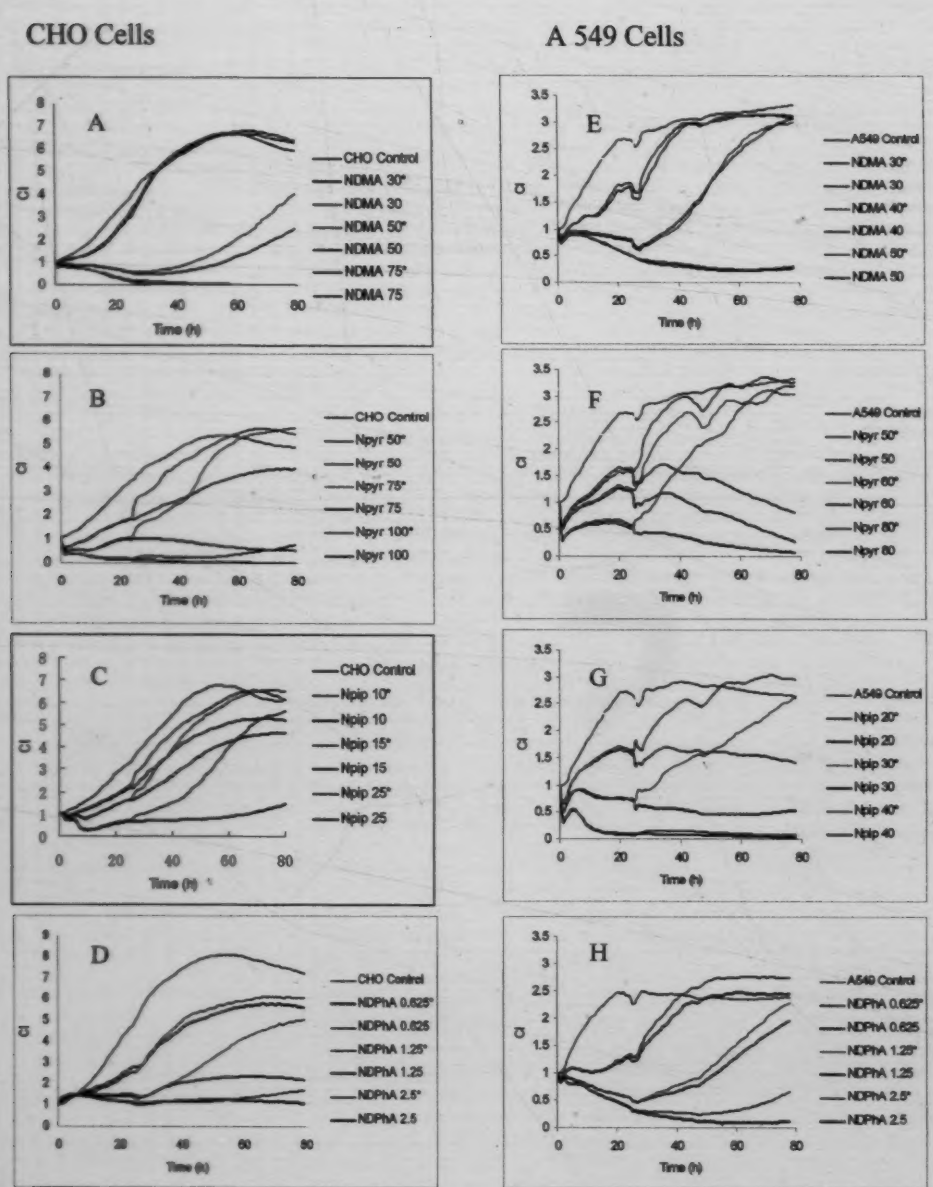

Figure 2-7. Reversibility study results of nitrosamines on CHO cells (A, B, C, D) and A549 cells (E, F, G, H).. After 24 h treatment with nitrosamines, the media containing nitrosamines were replaced by fresh media (*). The growth curves were compared with those of the control cells, whose media were not replaced.

The reversibility reveals the ability of cells to recover from chemically induced damage. The results indicated that the effects of exposure to NDMA and NDPhA for a short time are probably more persistent than those of exposure to NPip and NPyr.

2.3.6 Effects of Nitrosamines on CHO Cells:Cell-Killing and Cell Cycle Arrest

Based on the preliminary cytotoxicity results obtained from RT-CES, further investigation was conducted to determine the cytotoxic effects of nitrosamines with respect to cell-killing and cell cycle regulation. The Trypan blue staining assay was used on CHO-K1 cells treated with the $IC_{50(24\ h)}$ nitrosamine concentration (NDMA 35 mM, NPyr 40 mM, NPip 10 mM, and NDPhA 1.25 mM) to determine the amount of cell death induced by each nitrosamine. The results are shown in Figure 2-9.

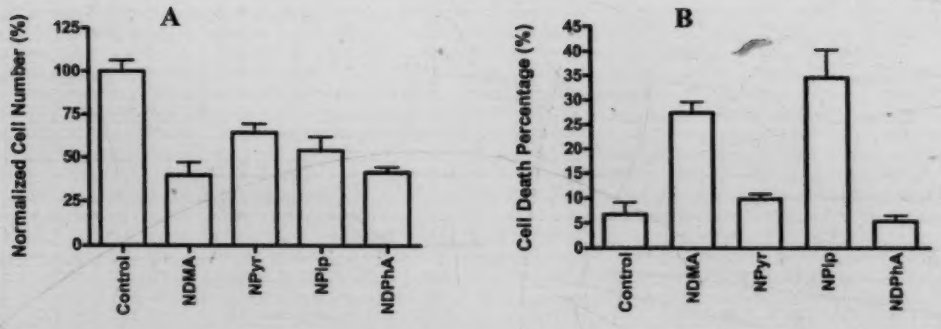

Figure 2-8. Measurement of cell death induction in CHO-K1 cells treated with four nitrosamines at IC_{50} at 24 h. CHO-K1 cells were treated with four nitrosamines at concentration of IC_{50} for 24 hrs, and then followed by Trypan blue staining. (A) Percentage of total (live + dead) number of cells after nitrosamine treatment normalized to cell control; (B) Percentage of dead cells after nitrosamine treatment. Error bars indicate one standard deviation.

Figure 2-8A compares the total cell numbers after treatment with different nitrosamines at IC_{50} concentrations, the results show a higher total cell number after treatment with NPyr and NPip compared to NDMA and NDPhA treatment (Figure 2-8A). Figure 2-8B compares corresponding percentages of dead cells. NDMA and NPip treatment resulted in higher numbers of dead cells indicating that induction of cell death is an important mechanism of cytotoxicity for NPip and NDMA. NPyr and NDPhA treatment did not induce significant cell death compared to the control. It is reasonable to

speculate that NDPhA and NPyr may affect the cells by inhibiting their growth rather than by killing them.

The effects of nitrosamines on cell cycle regulation were analyzed by flow cytometry after staining with propidium iodide. The distribution of CHO cells among the cell cycle stages was measured using flow cytometry following treatment with the IC_{50}(24 h) concentration (NDMA 35 mM, NPyr 30 mM, NPip 10 mM, and NDPhA 1.25 mM). The results of cell cycle analysis of the effects of nitrosamines on CHO cells are shown in Figure 2-9.

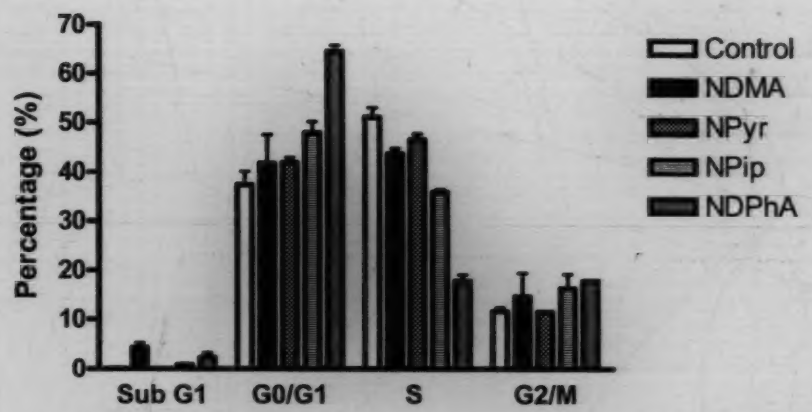

Figure 2-9. Cell cycle analysis of CHO cells after treatment with four nitrosamines. Percentage of cells in each particular cell cycle phase was analyzed by flow cytometry after 24 h treatment with each compound.

The proportions of control CHO cells distributed in G_0/G_1 and S phases were 37% and 51%. After treatment with NPip and NDPhA, CHO cells distributed in G_0/G_1 phase increased to 48 and 64%; only weak increases were observed in cells treated with NDMA and NPyr. Consistently, the proportion of cells treated with NPip and NDPhA treated in S phase decreased to 36% and 18%, respectively. These results indicate that NDPhA and NPip are capable of arresting considerable cells in G_0/G_1 phase, keeping the cells from entering the DNA synthesis phase. The cell cycle regulation effects of NDMA and NPyr are less significant.

Based on the information of the cell-killing effects and the cell cycle analysis results, the cytotoxicity characteristics of nitrosamines are summarized in Table 2-3.

Table 2-3. Summary of cytotoxicity of nitrosamines on CHO cells and the mechanistic information obtained from this study

Compounds	NDMA	NPyr	NPip	NDPhA
Cell-killing effect	+	-	++	-
Cell cycle arrest	+	+	++	+++
Reversibility	-	++	++	+
IC_{50} at 24 h (mM)	32.30	30.90	9.30	1.30

Our work demonstrated that the RT-CES system is a suitable technique for the detection of cytotoxicity in a high throughput, real-time, label-free manner. It is capable of detecting the chemical-dependent, dose-dependent, time-dependent, and cell-dependent cytotoxicity in one experiment. Another advantage of RT-CES is that it can provide additional information such as reversibility, which could produce mechanistic information with the help of other molecular biology techniques.

As each method has its own advantages and disadvantages, from our experience, the main limitations include: high cost of the disposable E-plates make this method relatively expensive; only attachable cells could be tested; and sometimes the morphological changes induced cell index decrease could not be differentiated from cell death.

Our work is the first to study the toxicity of four nitrosamine compounds on different cells with regard to risk and exposure pathway knowledge of DBPs. NDPhA, which was thought to be less potent in previous studies due to its lower genotoxicity, exhibits potent and less recoverable cytotoxicity. In addition, NDPhA shows a strong ability to arrest cells in G0/G1 phase and prevent them from entering into S phase. Cell cycle arrest also may result from DNA damage through regulation of cell cycle checkpoint related proteins, such as p53 and cyclin dependent kinase, leading to cell death. DNA damages such as this may be not observable by routine genotoxicity detection methods. These unique cytotoxic properties of NDPhA need to be further investigated. For the cytotoxicity of NPip, both cell-killing and cell cycle arrest plays an important role; the effect of NDMA results is mainly from cell-killing with a small part of due to G_0/G_1 arrest; and NPyr causes only a small cell cycle arrest effect without any cell-killing effect.

2.4 References

Anundi, I. and K. O. Lindros (1992). "Evidence for cytochrome P450 2E1-mediated toxicity of N-nitrosodimethylamine in cultured perivenous hepatocytes from ethanol treated rats." *Pharmacol Toxicol* **70**(6 Pt 1): 453-8.

Backer, L. C., D. L. Ashley, et al. (2000). "Household exposures to drinking water disinfection by-products: whole blood trihalomethane levels." *J Expo Anal Environ Epidemiol* **10**(4): 321-6.

Brady, J. F., F. Xiao, et al. (1991). "Effects of disulfiram on hepatic P450IIE1, other microsomal enzymes, and hepatotoxicity in rats." *Toxicol Appl Pharmacol* **108**(2): 366-73.

Charrois, J. W., M. W. Arend, et al. (2004). "Detecting N-nitrosamines in drinking water at nanogram per liter levels using ammonia positive chemical ionization." *Environ Sci Technol* **38**(18): 4835-41.

Choi, J. and R. L. Valentine (2002). "A kinetic model of N-nitrosodimethylamine (NDMA) formation during water chlorination/chloramination." *Water Sci Technol* **46**(3): 65-71.

Grogan, J., M. Shou, et al. (1995). "Cytochrome P450 2A1, 2E1, and 2C9 cDNA-expression by insect cells and partial purification using hydrophobic chromatography." *Biochem Pharmacol* **50**(9): 1509-15.

Mitch, W. A., A. C. Gerecke, et al. (2003). "A N-Nitrosodimethylamine (NDMA) precursor analysis for chlorination of water and wastewater." *Water Res* **37**(15): 3733-41.
Mitch, W. A. and D. L. Sedlak (2004). "Characterization and fate of N-nitrosodimethylamine precursors in municipal wastewater treatment plants." *Environ Sci Technol* **38**(5): 1445-54.

Negishi, T., T. Shiotani, et al. (1991). "The genotoxicities of N-nitrosamines in Drosophila melanogaster in vivo: the correlation of mutagenicity in the wing spot test with the DNA damages detected by the DNA-repair test." *Mutat Res* **252**(2): 119-28.

Nicoletti, I., G. Migliorati, et al. (1991). "A rapid and simple method for measuring thymocyte apoptosis by propidium iodide staining and flow cytometry." *J Immunol*

Methods **139**(2): 271-9.

Plewa, M. J., Y. Kargalioglu, et al. (2002). "Mammalian cell cytotoxicity and genotoxicity analysis of drinking water disinfection by-products." *Environ Mol Mutagen* **40**(2): 134-42.

Plewa, M. J., E. D. Wagner, et al. (2004). "Chemical and biological characterization of newly discovered iodoacid drinking water disinfection byproducts." *Environ Sci Technol* **38**(18): 4713-22.

Richardson, S. D., J. E. Simmons, et al. (2002). "Disinfection byproducts: The next generation." *Environmental Science & Technology* **36**(9):198 A-205 A.

Schreiber, I. M. and W. A. Mitch (2006). "Nitrosamine formation pathway revisited: the importance of chloramine speciation and dissolved oxygen." *Environ Sci Technol* **40**(19): 6007-14.

Schreiber, I. M. and W. A. Mitch (2006). "Occurrence and fate of nitrosamines and nitrosamine precursors in wastewater-impacted surface waters using boron as a conservative tracer." *Environ Sci Technol* **40**(10): 3203-10.

Shvemberger, I. N. (1967). "[Carcinogenic nitrosamines]." Vopr Onkol **13**(1): 97-105.

Uhl, M., C. Helma, et al. (2000). "Evaluation of the single cell gel electrophoresis assay with human hepatoma (Hep G2) cells." *Mutat Res* **468**(2): 213-25.

Wilkening, S., F. Stahl, et al. (2003). "Comparison of primary human hepatocytes and hepatoma cell line Hepg2 with regard to their biotransformation properties." *Drug Metab Dispos* **31**(8): 1035-42.

Wong, H. L., S. E. Murphy, et al. (2005). "Cytochrome P450 2A-catalyzed metabolic activation of structurally similar carcinogenic nitrosamines: N'-nitrosonornicotine enantiomers, N-nitrosopiperidine, and N-nitrosopyrrolidine." *Chem Res Toxicol* **18**(1): 61-9.

Zhao, Y. Y., J. Boyd, et al. (2006). "Characterization of new nitrosamines in drinking water using liquid chromatography tandem mass spectrometry." *Environ Sci Technol* **40**(24): 7636-41.

Chapter 3: Application of the RT-CES System on studies of Cytotoxic Effects Induced by Particulate Matter on Pulmonary Epithelial Cells and Mechanistic Studies

3.1 Introduction

Particulate matter, or PM, is the term for particles existing in the air, including dust, dirt, soot, smoke, and liquid droplets (Brunekreef and Forsberg 2005). Particulate matters can be divided further into PM_{10}, $PM_{2.5}$, ultrafine particles, and nano-particles according to their aerodynamic diameter. A large number of epidemiological, toxicological, and clinical studies have revealed that long-term exposure to airborne particulate matter is associated with increased incidence of respiratory allergy, cardiopulmonary mortality, risk of lung cancer, and developmental toxicity (Glinianaia, Rankin et al. 2004; Brunekreef and Forsberg 2005; Gao, Yu et al. 2005).

Though the US EPA enacted particulate matter standards in 1997, setting the annual $PM_{2.5}$ standard at 15 $\mu g/m^3$ and the annual PM_{10} standard at 50 $\mu g/m^3$ (EPA, 1997), recent studies found that ultrafine particles (UFP; < 0.1 μm in aerodynamic diameter) may pose more prominent impact on health, suggestting that the knowledge of PM is far from enough despite extensive research conducted (Delfino, Sioutas et al. 2005).

An in vitro cytotoxicity test is the most cost-effective method for pre-screening the cytotoxicity of PM because of the high cost and ethical issues associated with animal tests. However, most of the conventional cytotoxicity assays are colorimetric assays, and

the dark color of the particles and their low solubility in media may cause interference and limit the utilization of those methods.

Thus, the primary objective of this study was to develop, validate, and apply the previously discussed RT-CES method for testing the cytotoxicity of particulate matter, including quartz particles of different sizes and two particulate matter standard materials, SRM 1649a and SRM 2975. Quartz particles of different sizes are the most common occupational particles. SRM 1649a is a real sample that could serve as a representative of PM_{10}. SRM 2975 is standard reference material generated from diesel exhaust. The sizes of these two particle SRM are similar. Those particles represent the most common particulate matter people may encounter in environmental or occupational settings; they are selected to demonstrate the ability of the RT-CES method to test the cytotoxicity of various particulate matter.

Another objective was to investigate the mechanisms underlying quartz particle induced cell death on two human-derived lung alveolar epithelial cells (A549 and SK-MES-1 cells). Silicosis is a serious fibrotic lung disease associated with the inhalation and deposition of quartz particles (Rimal, Greenberg et al. 2005). The mechanisms underlying the initiation and progression of silicosis are not fully understood.

The role of apoptosis in fibrotic lung disease is a double-edged weapon. Apoptosis is a protective process that eliminates injured cells without stimulating an inflammatory response. On the other hand, excessive apoptosis may aggravate lung injury. One of the

consequences of apoptosis is the detachment of epithelial cells from the basement membrane, which could result in the exposure of the underlying membrane to toxic products in the alveolar spaces, such as oxidants, proteinases, and other inflammatory factors. Destruction of the alveolar walls and activation of fibroblast and collagen production could lead to fibrosis during the repair process (Martin, Hagimoto et al. 2005).

The association between apoptosis of lung epithelial cells and fibrotic diseases is supported by the finding that patients with idiopathic pulmonary fibrosis have increased levels of pulmonary epithelial cell Fas expression and apoptosis (Kuwano, Kunitake et al. 1996). Another study found that repeated administration of bleomycin will induce apoptosis and lung fibrosis in mice (Hagimoto, Kuwano et al. 1997), whereas mice lacking the Fas receptor (*lpr* mice) were resistant against bleomycine induced fibrosis (Kuwano, Hagimoto et al. 1999). Thus, apoptosis has been proposed as an important mechanism of action of pathogenesis of fibrosis.

Several studies have demonstrated that silica induces apoptosis in macrophage cells and T cells and in vivo (Borges, Lopes et al. 2002; Gozal, Ortiz et al. 2002; Santarelli, Recchioni et al. 2004). However, it is still unknown whether quartz particles cause apoptosis to alveolar epithelial cells, which are important target cells involved in the pathogenesis of pulmonary fibrosis.

To clarify these questions, the primary objectives of this study are: (1) To establish the RT-CES system as a suitable cytotoxicity detection system for assessing the

cytotoxicity of particulate matters. (2) To apply the RT-CES technique in the detection of the cytotoxic effects of a PM mixture (SRM 1649a and SRM 2975) and quartz particles of different sizes. (3) To establish a suitable respiratory in vitro model to detect low cytotoxic particulate matters. (4) To determine the differing roles of apoptosis in quartz-induced cytotoxicity between two in vitro alveolar epithelial models.

3.2 Materials and Methods

3.2.1 Cell Culture and Growth Conditions

Two different human lung epithelial cells, A549 (ATCC CCL-185; American Type Culture Collection, Manassas, VA) and SK-MES-1 (HTB-58; ATCC), were cultured in 10 cm cell culture Petri dish (Corning) at 37 °C with 5% CO_2 in RPMI1640 medium (Sigma), supplemented with 10% fetal bovine serum (Sigma) and 1% penicillin/streptomycin (Invitrogen). To harvest the cells, the cells were washed twice with 5 mL PBS buffer (pH 7.2), then the buffer was drained and 1 mL 0.25% Trypsin/EDTA (Invitrogen) was added for 3 min or until cells detached in sufficient numbers. Then, 5 mL RPMI 1640 medium was added by gentle pipetting until well mixed, and centrifuged for 3 min at 300 g. The supernatant was drawn off, the cell pellet was dispensed in fresh medium and diluted accordingly to desired concentration.

3.2.2 Particles and Chemicals

Two quartz particles in two sizes, Q 66 and Q 70, (the range of diameters of particles are 0.35–3.50 μm and 1.2–20.0 μm, respectively) were purchased from

Sigma-Aldrich Chemical Co. Urban dust standard reference material, SRM 1649a, and diesel exhaust particle standard reference material, SRM 2975, were purchased from National Institute of Standards and Technology (NIST, Gaithersburg, MD). Two quartz particles were addressed to the cells by being suspended thoroughly in the culture media to desired concentration; the urban dust and diesel exhaust particles were first dissolved in methanol to 200 and 50 mg/mL, respectively, then suspended in media to desired concentration. The particle suspension alone and the cell index of wells treated with methanol only were tested

3.2.3 Cytotoxicity Study by Using RT-CES System

Three thousand A549 cells and 10000 SK-MES-1 cells in 100 μl medium were seeded into the wells of E-plates and cellular growth was dynamically monitored using the RT-CES system. E-plates were kept in the cell culture incubator for around 24 h until the CI value increased to around 1. The E-plates were removed, the remained medium was drawn off, and 200 μL particle suspensions of different concentrations suspended in growth medium were added into each well. Cells without treatment and cells treated with corresponding concentrations served as the control. Based on the CI data obtained from RT-CES, further dose response analyses were conducted using GraphPad Prism software.

The cytotoxicity of quartz particles were also tested by a conventional viability assay, the acid phosphatase assay described previously (Serrou, Solassol et al. 1972). This assay utilizes the cells' own lysosomal acid phosphatase enzyme to relate enzymatic

activity to cell numbers (Yang, Sinai et al. 1996). The native phosphatase is used to remove phosphate esters from compounds and release them into cells to be used as material for new molecules. This enzyme can also hydrolyse exogenous substrate p-nitrophenylphosphate (pNPP) and generate chromogenic compounds, and thus could be used as a viability assay. After the hydrolysis reaction, the substrate pNPP releases p-nitrophenol and an inorganic phosphate; the reaction is stopped by the addition of NaOH at a given time and p-nitrophenolate is produced, a yellow colored product that absorbs at 405 nm and therefore can be detected (Yang, Sinai et al. 1996).

In performing the assay, A549 and SK-MES-1 cells were seeded on 96-well plates overnight 5000 and 10000 cells/well, and treated the following day with 100 µl of medium suspending quartz particles for 24 h. After treatment, the medium was removed and the cells were washed once with 200 µl of PBS and then with 100 µl of PBS buffer solution containing 0.1 M Na-acetate (pH 5.5). Then 1% (v/v) Triton X-100 and 10 mM *p*-nitrophenyl phosphate (phosphatase substrate pNPP) (all from Sigma) were added to make the cells permeable to the pNPP substrate solution. Following incubation for 1 hour at 37 °C, 10 µl of 1 M NaOH was added to each well to stop the reaction and the developed absorbance measured with a microplate reader (Bio-Rad, Mississauga, ON) at 405 nm. All data is expressed as cell numbers normalized to the control obtained with untreated cells, and expressed as a percentage.

3.2.5 Cell Cycle Analysis

DNA fragmentation was analyzed by flow cytometry using cell cycle analysis for subploid DNA content (Nicoletti, Migliorati et al. 1991). Cells were cultured in a 5 cm culture Petri dish. When the cells reached 60% confluence, the remaining medium was drawn off and replaced with 5 mL particle-containing suspension at different concentrations. twenty-four hours after treatment, the cells were trypsinized and washed off by PBS buffer, and centrifuged at 300 g for 3 min. The pellets were washed with 5 mL ice-cold PBS buffer and centrifuged as before. The cells were then fixed in 70% ethanol overnight at 4°C. The next day, the cells were washed with 5 mL ice-cold PBS and centrifuged for 3 min at 300 g. The cell pellets was resuspended within 1 mL propidium iodide staining solution which was made in our laboratory by addressing 0.1% Triton X-100 (VWR), 100 μg/ml RNase A (Sigma), and 330 μg/ml propidium iodide (Sigma Chemical Co.) in 100 mL PBS buffer. The mixture was incubated for 30 min at room temprature in a dark room. The cell cycle data were collected using a Becton and Dickinson FACScan™ (Mountain View, CA) and processed using Cell Quest™ software (Becton and Dickinson).

3.2.6 Caspase Inhibitor Study

To determine whether caspase proteins are involved in quartz-induced alveolar epithelial cell death, we examined the protective effects of a pan-caspase inhibitor, z-vad-fmk. We pretreated A549 and SK-MES-1 with 50 μM (final concentration)

z-vad-fmk for 2 h, and then added quartz suspension at different concentrations. Cytotoxicity assay and cell cycle analysis were conducted to compare the protective effects with the cells treated with particles only.

3.2.7 Electron Microscope Study

3.2.7.1 Scanning Electron Microscope Study

A549 cells and SK-MES-1 cells were treated with quartz particles (0.2 mg/mL and 0.1 mg/mL, respectively) for 1, 2, 4, 6, 8, 16, and 24 h, and pre-fixed in 2.5% glutaraldehyde in Millonig's buffer solution (pH 7.2) for 1.5 h at room temperature. After samples had been washed with the same buffer, they were post-fixed with 1% osmium tetroxide in the same buffer for 1.5 h. These samples were washed briefly in distilled water and dehydrated in a graded series of ethanol solutions (50%, 70%, and 90%, 10 min each grade) before the final two 10-min dehydrations with absolute ethanol. The samples then were dried in a critical-point dryer (SeeVac, FL) at 31 °C for 5 min and mounted on stubs for sputter-coating (a sputter-coater, Edwards, S150B, England) with gold. The samples were examined with a Hitachi scanning electron microscope S-2500 (Tokyo, Japan).

3.2.7.2 Transmitted Electron Microscope Study

A549 cells and SK-MES-1 cells were treated with quartz particles (0.2 mg/mL and 0.1 mg/mL, respectively) for 2, 6, and 20 h. They were pre-fixed in 2.5% glutaraldehyde in 0.2 M cacodylate buffer (pH 7.3) for 1.5 h and post-fixed with 1% osmium teroxide in

the same buffer for 1.5 h. The samples were dehydrated the same following the SEM sample preparation for dehydration. Then the samples were embedded in Spurr's resin and cured at 70 °C for 10 h. The ultrathin sections were stained with 4% uranyl acetate for 30 minutes and lead citrate for 5 min. Micrographs were taken at 75 kv with a Hitachi transmission electron microscope H-7000 (Tokyo, Japan).

3.2.8 MMP Assay

The mitochondrial membrane potential (MMP) was measured by flow cytometry with the lipophilic cationic probe 5,5',6,6'-tetrachloro-1,1',3,3'-tetraethylbenzimidazolcarbocyanine iodide (JC-1) (Sigma) staining. After the cells were treated with quartz particles for 2, 4, 6, and 8 h, JC-1 was added directly to the cell culture medium (1 μM final concentration) and incubated for 15 min at 37 °C. The medium was then replaced with PBS, and the cells were quantitated to detect J-aggregate fluorescence intensity by using a Becton and Dickinson FACScan™. Data analysis was processed using Cell Quest™ software (Becton and Dickinson).

3.3 Results

3.3.1 The linear Relationship Between the Cell Index and the Cell Number

To assess the utility of impedance measurement of cell index as a functional readout for cell numbers and cell growth, we evaluated the relationship between the cell index and cell numbers for different cells. A549 cells and SK-MES-1 cells at different starting numbers were seeded into microelectronic sensor wells (E-plates), and the cell

index was automatically recorded every hour to monitor the cell growth in the wells. Figure 3-1 shows the RT-CES response curves and the linear relationship between the cell index and the cell numbers for both cell lines of A549 (A, C) and SK-MES-1 (B, D).

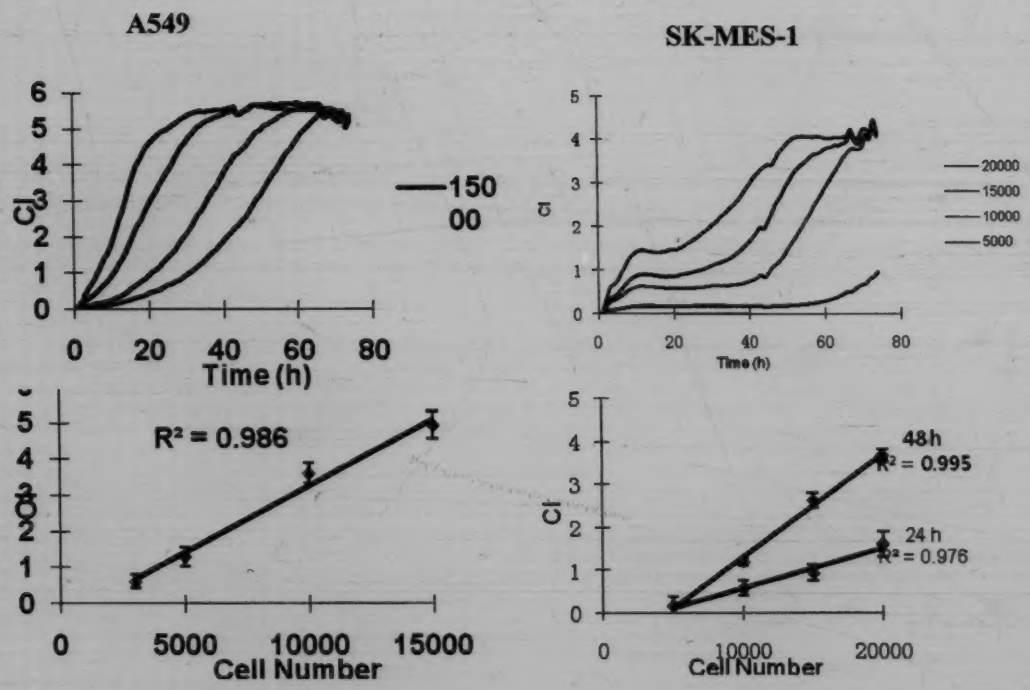

Figure 3-1. Cell quantification on the RT-CES system. The top panel shows the RT-CES growth curve of A549 and SK-MES-1 cells at different starting numbers ranging from 3000 to 20000. The slope of the growth curve indicates the different cell-specific growth rate. The lower panel shows the linear relationship between the cell index (CI) and the cell starting number 24 h or 48 h after plating.

Figure 3-1A shows the growth curves of A549 cells at different starting numbers ranging from 3000 to 15000. The cell index started with 0 in the beginning when no cells were attached to the electrodes embedded in the wells, and then increased gradually as the cells started attaching to the electrodes until it reached its maximum followed by a plateau phase as the cells covered the entire bottom area of the well. The slope of the curves represents the growth rate of the cells and the deeper the slope is, the faster the

cells grow. The greater the numbers of cells seeded, the shorter the time that the cell index needs to reach plateau phase. Figures 3-1C and D reveal the excellent linear relationship between the cell index and the starting cell numbers after 24 h from seeding of A549 cells and 24 and 48 h from seeding of SK-MES-1 cells. This means the cell index correlates not only with starting cell number but also with cell growth along a certain time period. The linear relationship before the cells reach the plateau phase allows us to measure quantitatively the cellular response to particulate matter exposure.

3.3.2 Measurement of Cellular Response of A549 and SK-MES-1 Cells after Quartz Particle Exposure

To investigate the applicability of the RT-CES technique to quantification of the particle induced cytotoxicity, we conducted an acid phosphatase assay, a conventional cytotoxicity assay, in parallel with the RT-CES method to measure the effects of quartz particles on A549 and SK-MES-1. For the RT-CES method, A549 and SK-MES-1 cells were plated in 16-well E-plates at 3000 and 10000 cells/well in 150 μL media. The cell index reflecting cellular growth was recorded automatically once every hour. After the cells attached to the electrodes and the cell index increased to 1 (approximately 24 h after seeding), the remaining media were replaced by 200 μL quartz particle suspensions at a range of concentrations from 0.003 to 0.8 mg/mL, and the cell index was monitored every hour for another 72 h.

The cross-sectional cell indexes at 12, 24, 36, 48, 60, and 72 h were exported to

GraphPad Prism software for further dose-response analysis, and IC_{50} values were derived for comparison of cytotoxicity. IC_{50} is the concentration of toxicants at which the cells need to exhibit 50% maximal cellular response; the lower the IC_{50} value, the more toxic the compound.

Figure 3-2 illustrates the result of the RT-CES method for detecting the cytotoxicity of quartz particles (size range 0.35 to 3.5 μm) on A549 (A, C) and SK-MES-1 (B, D) cells.

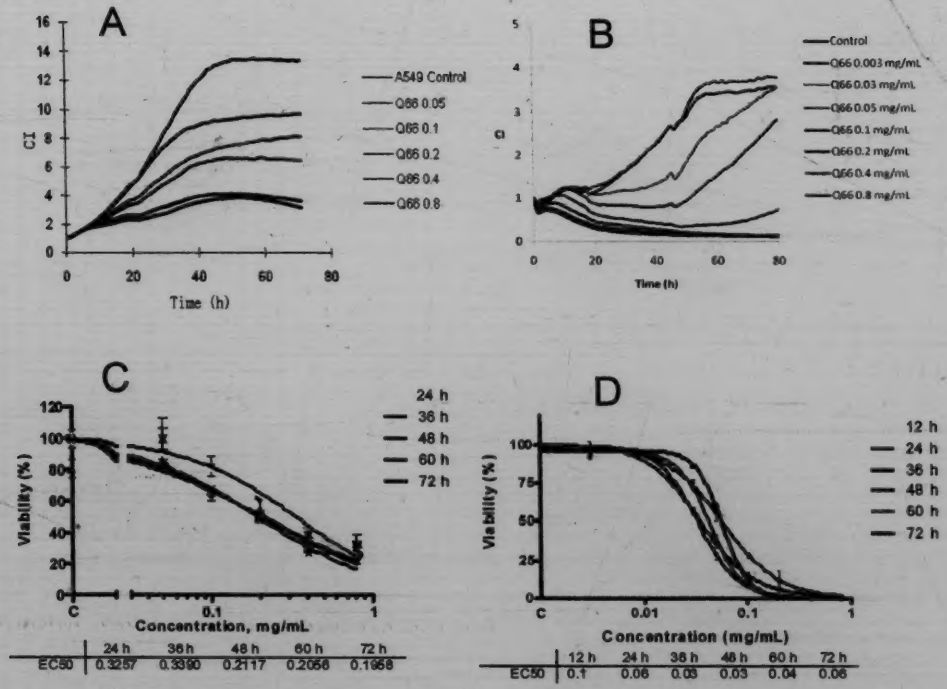

Figure 3-2. Dynamic monitoring of cytotoxic responses of A549 and SK-MES-1 cells in response to quartz particles. A and C are A549 cells, B and D are SKMES-1 cells. The control here indicates cells without quartz treatment. The cytotoxic response was monitored dynamically. The time-point zero indicates the time when the quartz particle suspension was added into the E-plate. The lower panel shows the dose-response analysis of quartz-induced cytotoxicity. The IC_{50} values at 12, 24, 36, 48, 60, and 72 h were recorded.

The cell index change of exposed A549 cells was dose-responsive for the concentrations ranging from 0.05 to 0.4 mg/mL. However, at quartz concentration of 0.8 mg/mL, the cell growth curve was almost at the same level as at concentration of 0.4 mg/mL. The lowest cell index at 72 h after exposure to 0.8 mg/mL quartz remained

around 3 (Figure 3-2 A). On the contrary, the cellular responses of SK-MES-1 cells are much more dose-responsive for the whole range of concentrations. The cell index dropped to zero at the concentration of 0.4 mg/mL, which means the cellular responses were 100% (Figure 3-2 B). The IC_{50} values at five time-points were derived from the consequent dose-response analysis and are shown in the bottom of the graph (Figures 3-2 C and D). However, the IC_{50} values for A549 cells may not reflect the real cytotoxic potency of quartz particles on A549 cells because of the lack of an available dose at which 100% response could be observed.

We compared the result obtained from the RT-CES system with that from the acid phosphatase assay. Also, to exclude the interference effect of quartz particles on the readout of both methods, we tested the signal generated by medium suspension containing quartz particles alone by both methods.

Figure 3-3 demonstrates the interference from particles in the acid phosphatase assay.

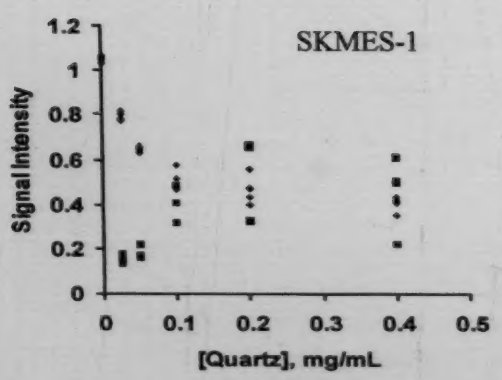

Figure 3-3. The interference of particles in the acid phosphatase assay. The interference from quartz particles in AP assay (n=4). Quartz particle suspension itself could generate considerable signal, indicated as blue dots; the corresponding total signals are expressed as red dots.

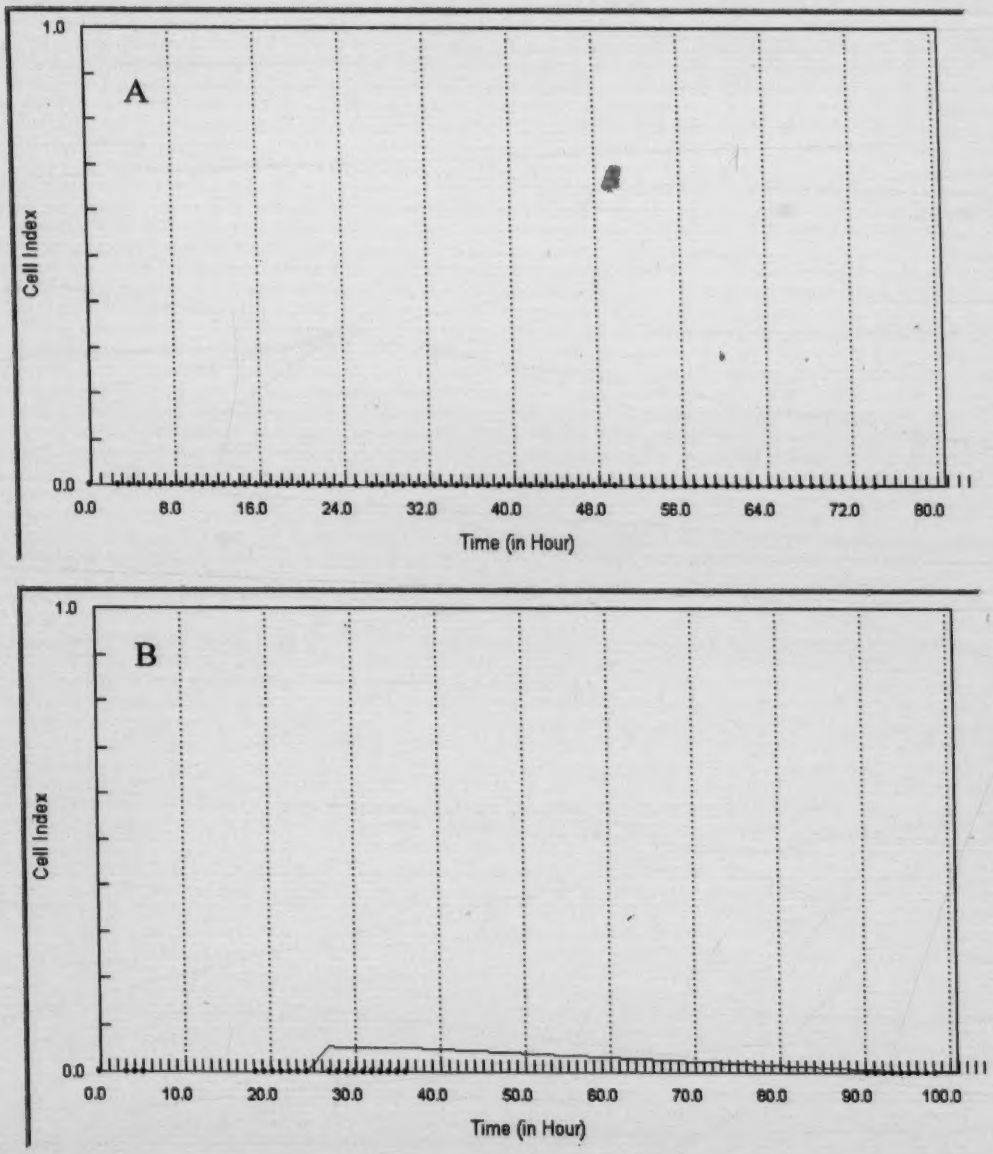

Figure 3-4. The interference from particles in the RT-CES method. A. time dependent signals from quartz particle of 200 mg/mL; B. time dependent signals from SRM 1649a (green) and SRM 2975 (red).

No signals were observed from the RT-CES system at all concentrations (original data shown in Figure 3-4), the cell index for entire experimental period kept being zero. While in the acid phosphatase assay, strong interference from particles was observed. The

signal intensity generated from the particles is quite high compared to the total signal obtained in the assay. Thus, colorimetric assays such as the AP assay, are not good methods for detection of particulate matter induced cytotoxicity.

3.3.3 Corresponding Morphological Changes Implicated by RT-CES Results.

The different patterns of the RT-CES response curves of A549 and SK-MES-1 cells may be related to the different patterns of morphological changes. To compare the morphological changes of both cells after quartz treatment, we treated A549 and SK-MES-1 cells with 0.2 and 0.1 mg/mL quartz particles for 8 h and 24 h. The morphological changes were observed using a scanning electron microscope. Figure 3-4 shows the distinct morphological changes on A549 cells and SK-MES-1 cells.

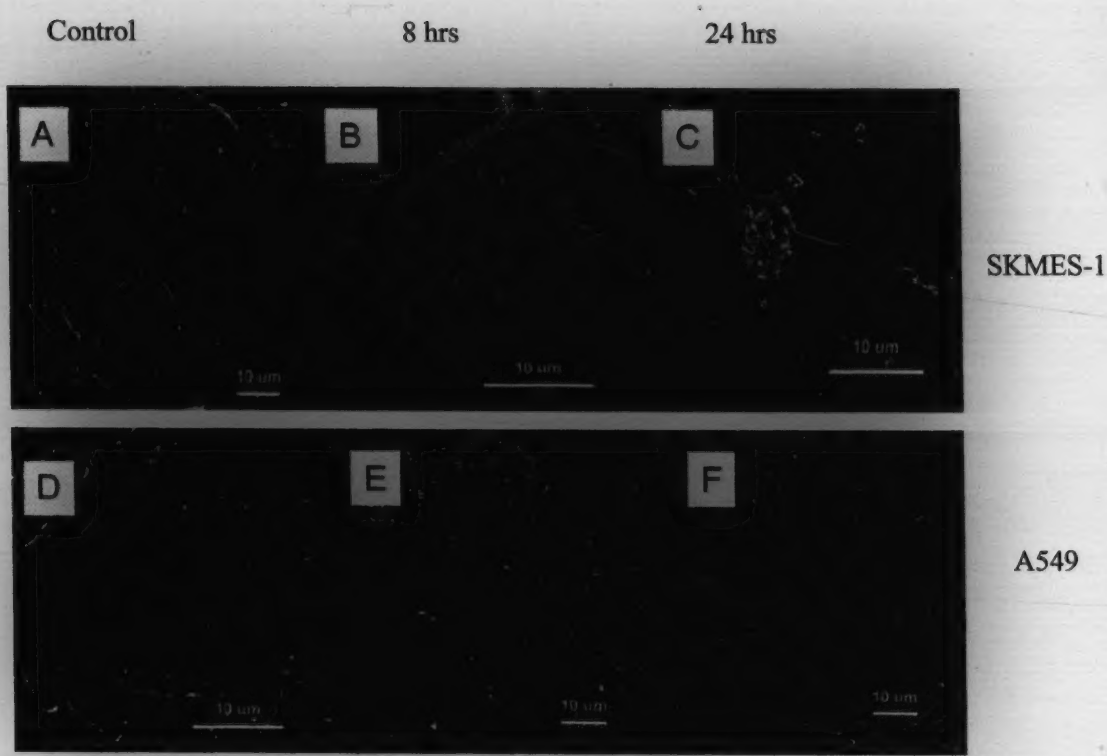

Figure 3-5. Corresponding morphological changes observed from scanning electron microscope study. A549 and SK-MES-1 cells are treated with 0.2 and 0.1 mg/mL quartz, respectively; the morphological changes were observed 8 and 24 h later. The top panel shows the morphological change of SKMES-1 cells. (A) control; (B) 8 hrs; (C) 24 hrs. The bottom panel demonstrate the results of A549 cells, (D) control; (E) 8 hrs; (F) 24 hrs.

The main changes of SK-MES-1 cells included cell blebbing, rounding and shrinkage. The diameter of the cell decreased to 5 μm after 24 h treatment compared to 30 μm of the control (Figures 3-4 A, B, C). Those morphological changes are the most important criteria for apoptosis. The morphological changes of A549 cells were not as

prominent as those of SK-MES-1 cells (Figure 3-4 D, E, F). A549 cells still retained their polyangular shape, and the size of the cells did not shrink dramatically; the evidences of cellular damage included the loss of normal microvilli on the surface and small lesions on the cells.

The morphological changes partly explain the results from the RT-CES system, which is based on the measurement of impedance changes induced by the interaction between cells and microelectronic sensors. Their well-maintained morphology allowed the A549 cells to remain attached to the electrodes and thus generate higher impedance. On the contrary, SKMES-1 cells rounded up and shrank in size, and their degree of attachment decreased, thus the cell index dropped more rapidly. The confirmed morphological changes also demonstrate the ability of the RT-CES system to monitor comprehensive biological changes including cell viability and morphological change resulting from particle exposure.

The morphological changes also reflect the underlying mechanisms of cytotoxicity. As cell membrane blebbing and cellular shrinkage are typical characteristics of apoptotic cell death, we examined the percentage of apoptotic cells by flow cytometry. The A549 and SK-MES-1 cells were treated with quartz particles for 24 h. The DNA subploid population was determined by staining with propidium iodide solution and measured by flow cytometry. The percentage of cells in sub G1 peak represents the percentage of apoptotic cells. Figure 3-5 demontrates the percentage of apoptosis in SK-MES-1 cells

treated with quartz particles compared to A549 cells. After exposure to 0.2 and 0.4 mg/mL quartz particles, 35% and 89% SKMES-1 cells were apoptotic, respectively, only 7% and 30% cells of A549 cells, respectively, l were distributed in subG1 peak.

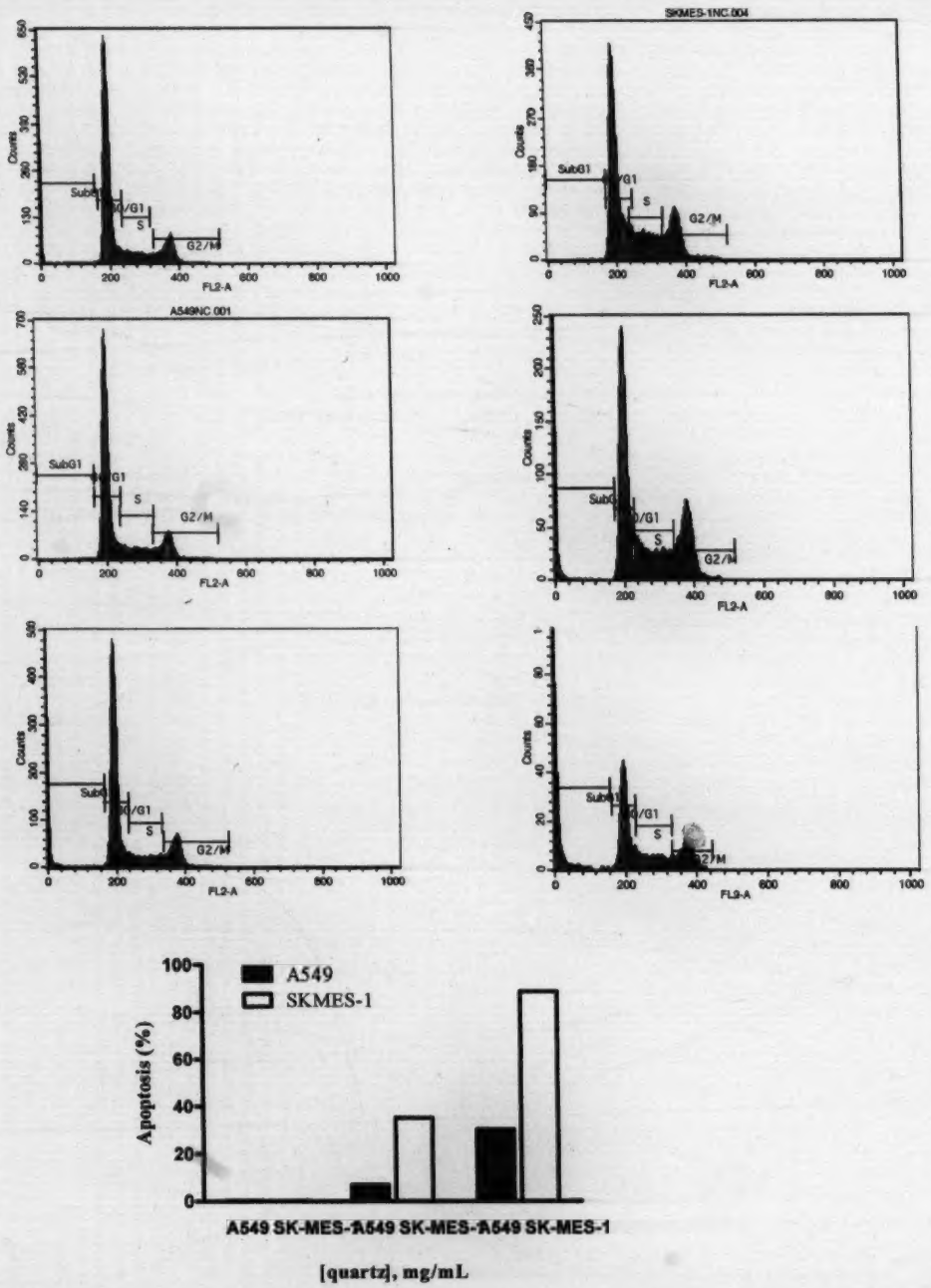

Figure 3-6. Subsequent flow cytometry study indicating the different mechanisms underlying different quartz induced A549 and SK-MES-1 cytotoxicity. A549 and SK-MES-1 cells were treated with 0.2 and 0.4 mg/mL quartz particle suspensions for 24 h. The percent of apoptotic cells in total cells were measured by flow cytometry. The solid bar represents A549 cells and the open bar represents SKMES-1 cells.

We performed a TEM study to observe cellular organelle changes during quartz

exposure. A549 cells and SK-MES-1 were treated with 0.2 mg/mL and 0.1 mg/mL quartz suspension for 2, 6, and 20 h, and then were fixed and embedded for TEM examination. As shown in Figure 3.6, A549 cells exhibited changes such as nuclear membrane rupture, cellular edema, and mitochondrial edema. SK-MES-1 cells demonstrated chromatin condensation, while the nuclear membrane remained intact. The increase in the number of mitochondria in SK-MES-1 cells implies the cells may initiate active metabolism and repair activities.

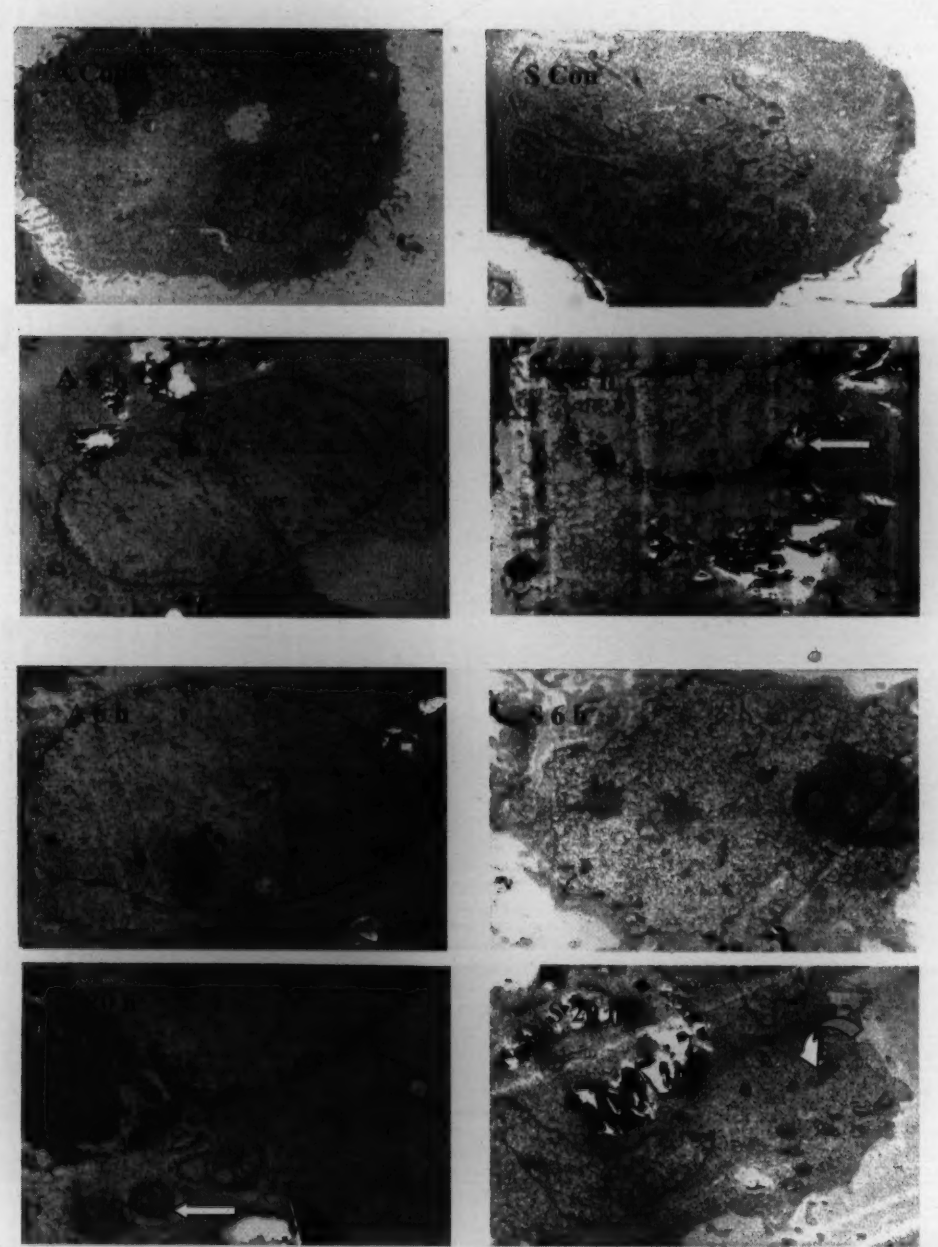

Figure 3-7. Transmission electron microscope study results demonstrate the cellular organelle morphological changes of quartz-induced alveolar epithelial cell death. For A549 cells, the changes include the rupture and discontinuity of nuclear membrane (solid arrow), and mitochondrial edema (open arrow). For SK-MES-1 cells, the nuclear membrane remained integrated while the chromatin condensed (open arrow) and the mitochondria increased in number while maintaining their structure (curve arrow).

3.3.4 Involvement of Caspases Evidenced by the Protective Effects of Caspase Inhibitor

To determine whether caspase protein is involved in quartz-induced alveolar epithelial cell death, we examined the protective effects of a pan-caspases inhibitor, z-vad-fmk. A549 and SK-MES-1 cells were pre-treated with 50 mM pan-caspase inhibitor for 2 h before quartz particles were added. The cytotoxicity was compared with cells treated with quartz alone. After 24 h, we conducted both cell viability analysis and cell cycle analysis. The results are shown in Figure 3-6: 50 mM z-vad-fmk protected SK-MES-1 cells from cell death about 7% (quartz concentration 0.1 mg/mL) to 10% (quartz concentration 0.2 mg/mL) over quartz dose ranging from 0.05 to 0.2 mg/mL; also, from the cell cycle analysis, 50 mM z-vad-fmk attenuated SK-MES-1 cell apoptosis (14% reduction at quartz concentration 0.1 mg/mL). In contrast, z-vad-fmk had negligible effects on A549 cells in terms of cell viability and apoptosis.

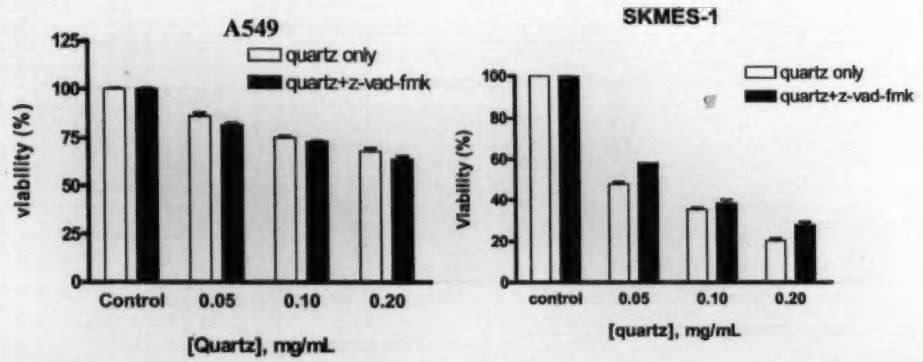

Figure 3-8. Results of viability assay comparing the protective effects of pan-caspase inhibitor from quartz induced cell death. The inhibitor protected SK-MES-1 cells from death by 7% to 10% but it had no effect on A549 cells. The viability is expressed as mean and standard error.

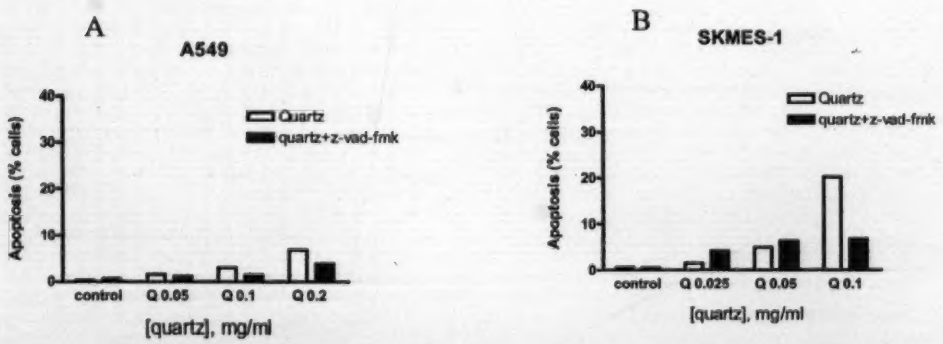

Figure 3-9. Cell cycle analysis results detecting the decrease of apoptosis cells after pre-treatment with caspase inhibitor. A. A549 without inhibitor, B. A549 with inhibitor, C. SK-MES-1 without inhibitor, D. SK-MES-1 with inhibitor. The caspase inhibitor decreased the apoptotic percentage in SK-MES-1 cells by 15% at 0.1 mg/mL quartz concentration, while for A549 cells, no obvious effects were observed.

Given the protective effects of the caspase inhibitor on quartz-induced SK-MES-1 cell damage, a specific role of caspase for quartz-induced SK-MES-1 cell apoptosis was suggested. However, no supporting evidence for the involvement of caspase for A549 cells was found in this study.

3.3.5 Quartz Induced Early MMP Change in SK-MES-1 Cells

The change in the mitochondrial membrane potential (MMP) is an early event in the regulation of the intrinsic apoptotic pathway (Bratton, Walker et al. 2001). We next assessed MMP changes in quartz-treated alveolar epithelial cells (Figure 3-8). A549 cells and SK-MES-1 cells were exposed to 0.2 and 0.1 mg/mL quartz at different time-points and the percentage of cells exhibiting loss of MMP was determined by flow cytometry following MMP sensitive dye JC-1 treatment. We used valinomycin as the positive control to ensure the quality of assay kit. The population of the cells located in the lower right quadrant indicates cells with damaged mitochondria and decreased membrane potential. In SK-MES-1 cells, the percentages of cells with damaged mitochondria are 7%, 17%, and 16 % at 2, 4, and 6 h respectively compared with 0.8% of the control; in A549 cells, the percentage of cells with MMP change were 1.2%, 0.6%, and 1.5 % respectively compared with 1.4% of the control.

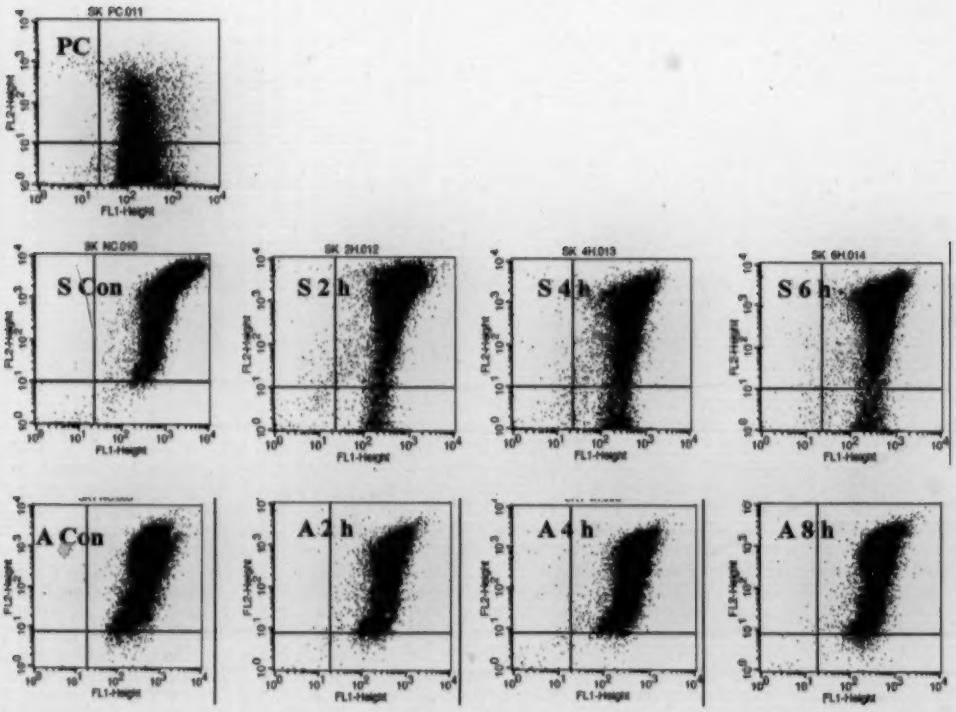

Figure 3-10. Results of MMP test evaluating mitochondrial damage which is an indicator of the intrinsic apoptotic pathway. The SK-MES-1 cells demonstrate mitochondrial membrane potential decrease by 7% as early as 2 h after quartz exposure, and increase to 17% at 4 h after exposure. The A549 cells did not exhibit obvious changes in MMP compared with control.

3.3.6 Application of RT-CES Technique in Biomonitoring the Cytotoxicity of Different Particles.

To apply the RT-CES technique in biomonitoring the cytotoxicity of particulate matter, we tested the cytotoxic effects of four particles on A549 and SKMES-1 cells. Figures 3-10 and 3-11 show the resulting RT-CES response curves. As we observe in Figure 3-10, for A549 cells, the minimal cell index towards quartz particles (A and B) is

not 0. For particle SRM 2975 (C), the dose response relationship is reversed. The highest concentration induced the highest cell index, and as the concentration decreased, the cell index decreased, while the cell index of particle control remained to be zero. Only particle SRM 1649a demonstrated evenly distributed cell growth curves at each particle concentration. Based on our results, A549 cells are not suitable as a sensitive in vitro model for detection of the cytotoxicity of environmental PM. The SK-MES-1 cells demonstrated much more sensitive and dose-responsive cytotoxic effects from the four particles. Further dose-response analysis was conducted.

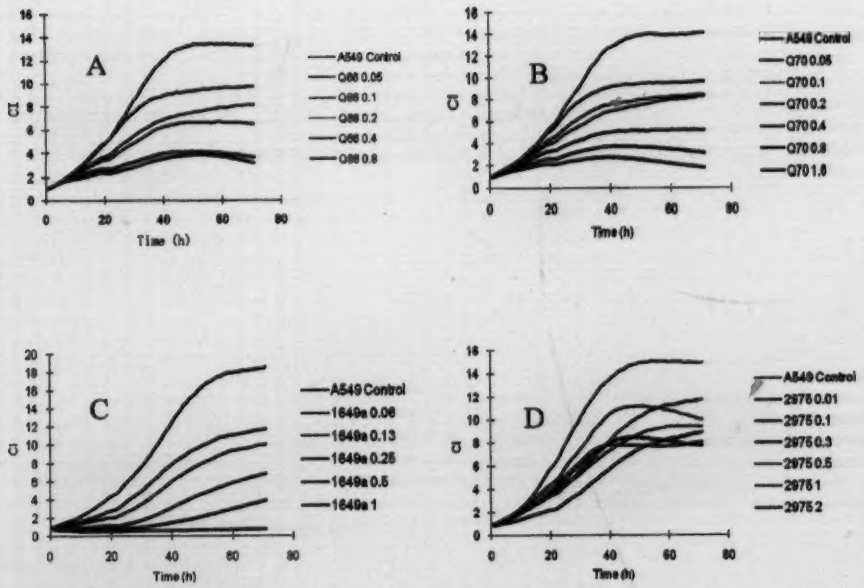

Figure 3-11. Cytotoxic effects of four particles on A549 cells
A. Quartz Q66 (diameter: 0.35–3.5 μm), B. Quartz Q70 (diameter 1.2–20 μm), C. SRM 1649a, and D. SRM 2975 on A549 cells.

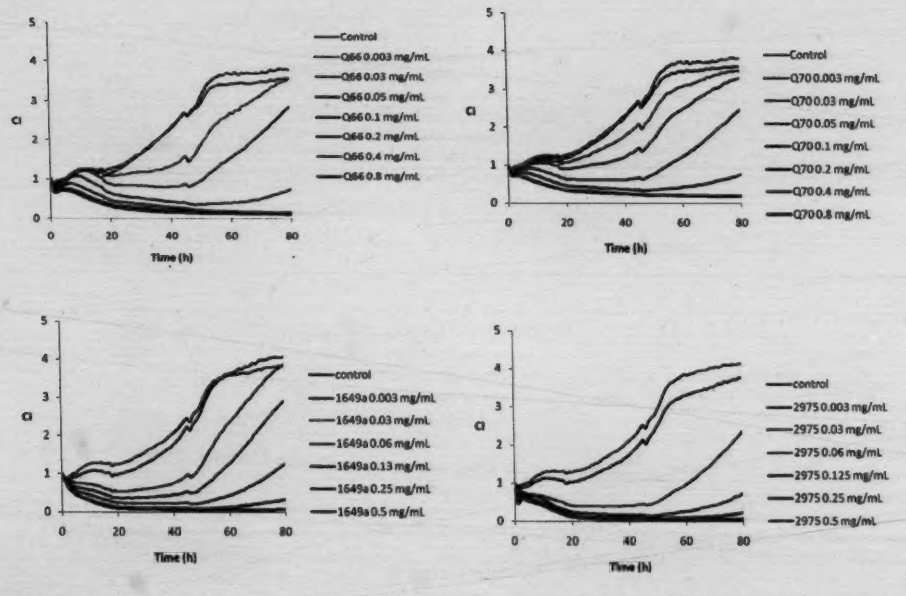

Figure 3-12. The effects of quartz Q66, quartz Q70, SRM 1649a, SRM 2975 on SKMES-1 cells.

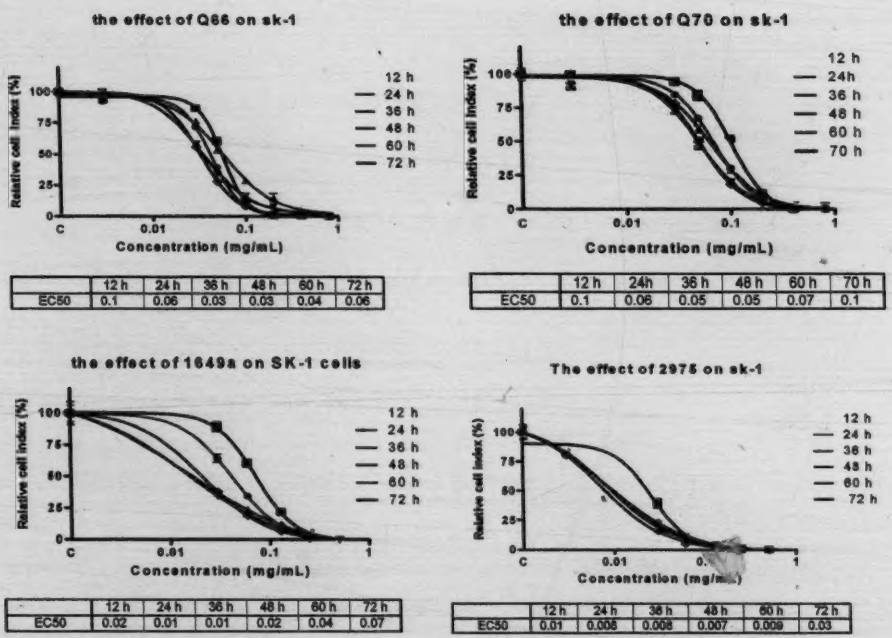

	12 h	24 h	36 h	48 h	60 h	72 h
EC50	0.1	0.06	0.03	0.03	0.04	0.06

	12 h	24h	36 h	48 h	60 h	70 h
EC50	0.1	0.06	0.05	0.05	0.07	0.1

	12 h	24 h	36 h	48 h	60 h	72 h
EC50	0.02	0.01	0.01	0.02	0.04	0.07

	12 h	24 h	36 h	48 h	60 h	72 h
EC50	0.01	0.008	0.008	0.007	0.009	0.03

Figure 3-13. Results of dose-response analysis for particle induced cytotoxicity on SK-MES-1 cells. The IC_{50} values at different time-points are displayed.

Subsequently, we conducted dose-response analysis for the cytotoxic effects of particles on SK-MES-1 cells. As the RT-CES system recorded the cellular responses every hour providing a high volume of data, theoretically, the IC50 at every hour could be calculated. As shown in Figure 3-12, we listed the IC50 at six time-points, 12, 24, 36, 48, 60, and 72 h. however, as the cell index are correlating with cell number only at log phase, the control cells may reach to plateau phase at 60 h and 72 h, thus the difference between the cell index between control and treated cells are minimized, thus the IC_{50} at 60 and 72 h may not accurately reflect the adverse effects of particles posed on cells. The rank order of cytotoxicity of the tested particles at 24 h was: SRM 2975 > SRM 1649a > Q66 > Q70.

3.4 Discussion

Particulate matter refers to materials suspended in the air in the form of minute solid particles or liquid droplets with other deteterious chemicals, for example, polyaromatic hydrocarbons (PAHs), sulfates, and nitrates, usually adsorbed on their surface (Brunekreef and Forsberg 2005). Exposure assessment and toxicity measurement are considerably difficult because of the highly complex chemical composition. The relative potency of particulate matter and underlying mechanisms still remain unclear in spite of extensive researches been conducted for decades past.

Cytotoxicity assays are rapid, sensitive, and inexpensive methods of toxicity screening and characterization of environmental agents that avoid the high costs and ethical issues associated with animal tests. Standardized cytotoxicity assays have become one of the criteria for toxicity characterization of environmental toxicants and provide lines of evidence for evidence-based regulation of those toxicants. However, for particulate matter, few cytotoxicity data are available due to some inherent technical limitations of current conventional colorimetric cytotoxicity assays.

In this study, we demonstrated the application of a novel label-free, dynamic, real-time cytotoxicity detection method for monitoring the cytotoxic effects of different particles on human alveolar epithelial cells. The RT-CES method is based on the alteration of impedance of cells from their interaction with microelectrodes that are

embedded in the bottom of microwell chips. The impedance signal is proportional to the morphological and viability changes. To demonstrate the capability of this technique for cytotoxicity evaluation of particulate matter, we tested quartz particles of different sizes (Q 66 and Q 70) and two standard reference materials (SRM 1649 and SRM 2975) on two human derived alveolar epithelial cells and ranked the cytotoxicity of those particles based on our results.

Jalava et al. tested the cytotoxicity of SRM 1649a and its ability to generate cytokines with and without methanol treatment. Low cytoxicity and no significant modification effects were observed with methanol treatment (Jalava, Salonen et al. 2005). SRM 2975 has been reported to be non-cytotoxic to human alveolar macrophage cells at all concentrations tested using the MTT test (Mundandhara, Becker et al. 2006). The MTT method determines the viability of cells by measuring the colorimetric changes associated with the amount of purple formazan crystals formed by reducing yellow tetrazolium salt in metabolically active cells. However, SRM 2975 remained insoluble and dark, the particle suspension itself generated intensive signals in the particle-containing medium controls, and the colorimetric changes due to cellular metabolism were relatively low; thus, the readout signals could not reflect the cellular viability changes.

The RT-CES method utilized the biological electrical impedance as the source of signal, and thus could eliminate colorimetric interference and generate reliable response

curves. The particle suspension controls did not generate any CI signals and the change of CI responsed to particle exposure in a time-dependent and dose-dependent manner. Thus, the RT-CES method is a suitable cytotoxicity screening method for cytotoxicity evaluation of particulate matter.

The responses of A549 and SK-MES-1 cells to exposure of PM are different. A549 cells are more sensitive to low concentration of particles relative to high concentration. Thus, the cytotoxicity would be overestimated if we use data from A549 to calculate IC_{50}s for comparison because the insensitive responses to particles at high concentration will mask the sensitive response to particles at low concentration. In response to SRM 2975, the relationship of the responses of A549 cells to particle concentration is inverted: the lower the concentration, the higher the response. Thus, the results obtained from A549 cells are not suitable for subsequent dose-response analysis.

SK-MES-1 cells are more sensitive than A549, and the CI index changes are more evenly distributed in all the dose ranges for every particle. The IC_{50}s were calculated to rank order the relative potency of particles. The rank order of cytotoxicity at 24 h after exposure is: SRM 2975 > SRM 1649a > Q66 > Q70. These results demonstrate that SK-MES-1 cell is a suitable in vitro model for cytotoxicity screening of particulate matter.

It is noteworthy that a large number of cytotoxicity studies of particles demonstrated that SRM 2975 and SRM1659a have low cytotoxicity or are non-cytotoxic

despite the high mass concentration of PAHs and toxic transitional metals adsorbed onto the particles (Singh, DeMarini et al. 2004; Jalava, Salonen et al. 2005; Musafia-Jeknic, Mahadevan et al. 2005). However, many studies demonstrated that these particles are probably carcinogenic and possess a strong capability to generate ROS and proinflammatory cytokines (Musafia-Jeknic, Mahadevan et al. 2005; Mundandhara, Becker et al. 2006). The discrepancy between the low cytotoxicity detected and the strong metabolic activity may be due to insensitive in vitro models used and lack of appropriate cytotoxicity detection assays. Methanol treatment of particles have been proven to have no significant impact on cytotoxicity and the release of proinflammatory factors (Jalava, Salonen et al. 2005); our study is in agreement with this finding. Further mechanistic studies regarding cytotoxicity induced by DEP and urban dust are needed.

Another objective of this study was to study the role of apoptosis in quartz-induced alveolar epithelial cell death. Apoptotic cell death induced by quartz particles has emerged as a important mechanism underlying silicosis. Although apoptosis was demonstrated in vitro in pulmonary macrophage cells, endothelial cells, and lymphocytes (Borges, Lopes et al. 2002; Santarelli, Recchioni et al. 2004; Thibodeau, Giardina et al. 2004), the role of apoptosis in quartz-induced alveolar epithelial cell death as well as the mechanism of apoptosis still remain unclear. Many researchers suggested a role of alveolar epithelial cell apoptosis in the induction and progression of pulmonary fibrosis which is also the typical pathogenic manifestation in silicosis (Hagimoto, Kuwano et al.

1997; Martin, Hagimoto et al. 2005), but few studies directly addressed whether quartz particles cause alveolar epithelial cells to undergo apoptosis.

In this study, we demonstrated that quartz particles caused type I alveolar epithelial cell (SK-MES-1) apoptosis in a dose-dependent fashion, while in type II (A549) cells, the role of apoptosis in quartz-induced cell death is not obvious. This is the first study that we are aware of that demonstrates that quartz causes apoptosis of alveolar epithelial cells. Apoptosis of SK-MES-1 cells after exposure to the quartz particles was evident by scanning electron microscope observation (Figure 3-4) Quartz-induced SKMES-1 apoptosis was evident in multiple independent assays including cell cycle analysis, morphological observation conducted by both scanning electron microscope and transmission electron microscope, and pan-caspase inhibitor study.

Apoptosis and necrosis are two distinct but interchangeable cell death modes. Though there are several available assays, such as flow cytometry, morphological observation, TUNEL staining, DNA gel electrophoresis, and annexin V staining assay, that are claimed to be able to differentiate these two types of cell death, each of them separately is considered unable to unambiguously distinguish apoptosis and necrosis. Some studies revealed that early necrosis sometimes shares some common initiation features with apoptosis such as the external expose of phosphatidylserine (Lecoeur, Prevost et al. 2001), thus flow cytometry analysis after annexin V and propidium iodide staining is not a definite assay. Internucleosomal break of DNA and the generation of

"ladder"-like DNA fragments with 180 bp multiples has also been considered a characteristic feature of apoptosis whereas the cleavage of DNA in necrotic cells occurs at random and generates diffused marks in agar gel. However, apoptosis of some cells may occur without internucleosomal DNA fragmentation (Cohen, Sun et al. 1992) and it is difficult to detect DNA ladders if the numbers of apoptotic cells are small.

The morphological changes are considered as the most solid evidence to determine cell death modes (Rello, Stockert et al. 2005). The main morphological characteristics of apoptosis include membrane blebbing, severe shrinkage, and detachment from substrate (Cohen, Sun et al. 1992). The studies of morphological changes of necrosis are relatively rare; cellular edema and membrane disintegrity are the main features of necrosis (Rello, Stockert et al. 2005). From these criteria, SEM observation provided evidence of apoptosis in quartz-treated SK-MES-1 cells and TEM observation demonstrate that A549 cells exhibited morphological changes of necrosis such as rupture of cellular and nuclear membranes, the mitochondrial edema and loss of normal cristae structure which could be easily seen in normal cells.

Mitochondria have a critical role in regulating apoptosis by diverse apoptogenic agents. Early changes in mitochondrial function are important for initiation of the intrinsic apoptotic process (Green and Reed 1998; Brenner and Kroemer 2000). In this study, after confirming the different cell death modes in two alveolar epithelial cells, we explored whether quartz caused mitochondrial dysfunction to induce apoptosis.

quartz-induced decreases in SK-MES-1 cell mitochondrial membrane potential is an early event, since abnormalities were noted as early as 2 h after quartz exposure which is correlated with the early morphological changes. The mitochondrial membrane potential change in SK-MES-1 cells implies linkage between mitochondria damage and apoptosis; this finding is in agreement with another study which suggests quartz-induced apoptosis on alveolar macrophages relies on mitochondrial integrity (Thibodeau, Giardina et al. 2003). However, the mechanisms involved in this process are not revealed in this study.

To date, there is limited literature that discusses directly silica-induced apoptosis of alveolar epithelial cells to our knowledge (Lim, Kim et al. 1999). Most apoptosis studies about quartz particles focus on the impact on alveolar macrophages. It is interesting to note that there is much more research on the effect of asbestos, another environmental pulmonary fibrogenic agent, on alveolar epithelial cells. Most studies choose A549 cells as corresponding in vitro counterpart of alveolar epithelial cells. It is reasonable to speculate that if some environmental agents cause type I alveolar epithelial cells instead of type II alveolar epithelial cells, it will be difficult to detect using A549 cells as the in vitro model because A549 cells are more similar to type II alveolar epithelial cells rather than type I alveolar epithelial cells.

The major finding of this study is that the RT-CES method is a reliable label-free, real-time method for testing of the cytotoxicity of environmental contaminants, especially for particles which are usually hard to detect by traditional colorimetric viability assays.

We also first demonstrated that SK-MES-1 cells are a sensitive and reliable in vitro model in response to particle exposure. A549 cells, which are widely used as the in vitro model in pulmonary toxicity studies, are not sensitive enough for assessment of the cytotoxicity of particles with low cytotoxicity. In addition, SK-MES-1 cells are similar to type I alveolar epithelial cells. Type I alveolar epithelial cells form the structure and account for more than 90% of the alveoli. The destruction of those cells will damage the integrity of the alveolar membrane and cause physiopathologic disorders. However, studies involving type I alveolar cell damage lag behind those of type II cell damage because of lack of molecular markers. By comparing the IC_{50}s from SK-MES-1 cells, the rank order of the four environment relevant particles of our study is SRM 2975 > SRM 1649a > Q66 > Q70.

The subsequent mechanism studies of quartz-induced alveolar epithelial cell damage revealed that quartz of respirable size may induce apoptosis in type I alveolar epithelial cells which was evidenced by several different assays. It is reasonable to speculate that apoptosis of type I alveolar epithelial cells may further damage the alveolar membrane and expose underlying tissue to inflammatory molecules and other cytokines that will cause lung injury. The change of type II alveolar epithelial cells is more likely necrosis, which is uncontrolled passive cell death. Consequent rupture and release of cytoplasm and cell transduction molecules will incur an inflammatory response and activation of macrophage cells will then lead to secondary injuries and silicosis.

3.5 References

http://www.epa.gov/ttn/oarpg/naaqsfin/pmfact.html

Borges, V. M., M. F. Lopes, et al. (2002). "Apoptosis underlies immunopathogenic mechanisms in acute silicosis." *Am J Respir Cell Mol Biol* **27**(1): 78-84.

Bratton, S. B., G. Walker, et al. (2001). "Recruitment, activation and retention of caspases-9 and -3 by Apaf-1 apoptosome and associated XIAP complexes." *Embo J* **20**(5): 998-1009.

Brenner, C. and G. Kroemer (2000). "Apoptosis. Mitochondria--the death signal integrators." *Science* **289**(5482): 1150-1.

Brunekreef, B. and B. Forsberg (2005). "Epidemiological evidence of effects of coarse airborne particles on health." *Eur Respir J* **26**(2): 309-18.

Cohen, G. M., X. M. Sun, et al. (1992). "Key morphological features of apoptosis may occur in the absence of internucleosomal DNA fragmentation." *Biochem J* **286 (Pt 2)**: 331-4.

Delfino, R. J., C. Sioutas, et al. (2005). "Potential role of ultrafine particles in associations between airborne particle mass and cardiovascular health." *Environ Health Perspect* **113**(8): 934-46.

Gao, X., Q. Yu, et al. (2005). "Health effects of airborne particulate matter trace elements." *Biomed Environ Sci* **18**(5): 349-55.

Glinianaia, S. V., J. Rankin, et al. (2004). "Particulate air pollution and fetal health: a systematic review of the epidemiologic evidence." *Epidemiology* **15**(1): 36-45.

Gozal, E., L. A. Ortiz, et al. (2002). "Silica-induced apoptosis in murine macrophage. Involvement of tumor necrosis factor-a and nuclear factor-kB activation." *American Journal of Respiratory Cell and Molecular Biology* **27**(1): 91-98.

Hagimoto, N., K. Kuwano, et al. (1997). "Apoptosis and expression of Fas/Fas ligand mRNA in bleomycin-induced pulmonary fibrosis in mice." *Am J Respir Cell Mol Biol* **16**(1): 91-101.

Jalava, P., R. O. Salonen, et al. (2005). "Effects of sample preparation on chemistry, cytotoxicity, and inflammatory responses induced by air particulate matter." *Inhal Toxicol* **17**(2): 107-17.

Kuwano, K., N. Hagimoto, et al. (1999). "Essential roles of the Fas-Fas ligand pathway in the development of pulmonary fibrosis." *J Clin Invest* **104**(1): 13-9.

Kuwano, K., R. Kunitake, et al. (1996). "P21Waf1/Cip1/Sdi1 and p53 expression in association with DNA strand breaks in idiopathic pulmonary fibrosis." *Am J Respir Crit Care Med* **154**(2 Pt 1): 477-83.

Lecoeur, H., M. C. Prevost, et al. (2001). "Oncosis is associated with exposure of phosphatidylserine residues on the outside layer of the plasma membrane: a reconsideration of the specificity of the annexin V/propidium iodide assay." *Cytometry* **44**(1): 65-72.

Lim, Y., J. H. Kim, et al. (1999). "Silica-induced apoptosis in vitro and in vivo." *Toxicology Letters* **108**(2-3): 335-339.

Martin, T. R., N. Hagimoto, et al. (2005). "Apoptosis and epithelial injury in the lungs." *Proc Am Thorac Soc* **2**(3): 214-20.

Mundandhara, S. D., S. Becker, et al. (2006). "Effects of diesel exhaust particles on human alveolar macrophage ability to secrete inflammatory mediators in response to lipopolysaccharide." *Toxicol In Vitro* **20**(5): 614-24.

Musafia-Jeknic, T., B. Mahadevan, et al. (2005). "Long-term effects of a standardized complex mixture of urban dust particulate on the metabolic activation of carcinogenic polycyclic aromatic hydrocarbons in human cells in culture." *Toxicol Sci* **88**(2): 358-66.

Nicoletti, I., G. Migliorati, et al. (1991). "A rapid and simple method for measuring thymocyte apoptosis by propidium iodide staining and flow cytometry." *J Immunol Methods* **139**(2): 271-9.

Rello, S., J. C. Stockert, et al. (2005). "Morphological criteria to distinguish cell death induced by apoptotic and necrotic treatments." *Apoptosis* **10**(1): 201-8.

Rimal, B., A. K. Greenberg, et al. (2005). "Basic pathogenetic mechanisms in silicosis:

current understanding." *Curr Opin Pulm Med* **11**(2): 169-73.

Santarelli, L., R. Recchioni, et al. (2004). "Crystalline silica induces apoptosis in human endothelial cells in vitro." *Cell Biology and Toxicology* **20**(2): 97-108.

Serrou, B., C. Solassol, et al. (1972). "[Cell viability and lysosomal enzymes]." *Nouv Presse Med* **1**(2): 109.

Singh, P., D. M. DeMarini, et al. (2004). "Sample characterization of automobile and forklift diesel exhaust particles and comparative pulmonary toxicity in mice." *Environ Health Perspect* **112**(8): 820-5.

Thibodeau, M. S., C. Giardina, et al. (2004). "Silica-Induced Apoptosis in Mouse Alveolar Macrophages Is Initiated by Lysosomal Enzyme Activity." *Toxicological Sciences* **80**(1): 34-48.

Yang, T. T., P. Sinai, et al. (1996). "An acid phosphatase assay for quantifying the growth of adherent and nonadherent cells." *Anal Biochem* **241**(1): 103-8.

Chapter 4: Summary and Future Work

A RT-CES technique was successfully developed for high throughput detection of cytotoxicity of environmental chemical and particulate contaminants. It can provide semi-quantitative measurement of cytotoxicity, and with specific experimental design, it can indicate differences in underlying mechanisms to direct further investigations.

We successfully used the RT-CES technique to study the cytotoxicity of new drinking water disinfection by-products. We obtained unique cytotoxicity information for four N-nitrosamine compounds (NDMA, NPyr, NPip and NDPhA) on four mammalian and human cell lines (CHO, A549, T24, and HepG2). The T24 cells, a human bladder cancer cell line, are the most sensitive towards nitrosamine exposure; NDPhA causes the most cytotoxicity among the four nitrosamine compounds.

We further demonstrated the capability of the RT-CES method for evaluation of the reversibility of cytotoxicity after nitrosamine treatments. The results show that different nitrosamines may go through different pathways to cause cytotoxicity: NDMA and NPip tend to kill the cells whereas NDPhA and NPyr tend to inhibit the cell growth instead of killing the cells. The subsequent cell cycle analysis also demonstrates that different nitrosamines cause various levels of cell cycle inhibition. NDPhA is the most potent inhibitor of the cell cycle, suggesting that its toxicity should not be ignored as previously assumed. Cell cycle regulation is the most crucial in the fetal development and aging as

well as the generation of cancer. In order to seek the causal link between disinfected drinking water consumption and fetal developmental failures, further studies on nitrosamines could focus on the effects of nitrosamines on neuron differentiation and development.

Having demonstrated the cytotoxicity of chemicals by the RT-CES technique, we further developed the technique for testing particulate matter: two quartz particles of different sizes and standardized urban dust (SRM 1649a) and standardized diesel exhaust particles (SRM 2975) on two human lung cancer cell lines (A549 and SK-MES-1). Our results reveal that SK-MES-1 cells are more sensitive than A549 cells and that their dose-response curves are more evenly distributed. Although A549 cells are more often used as the in vitro model in pulmonary toxicity studies, we observed that it is not the best model for testing particulates. A large portion of the literature demonstrates little or no cytotoxity of particulate matter because of lack of sensitive detection methods. Our results suggest that SK-MES-1 cells are more suitable and practical to measure and compare the cytotoxicity of particulate matter.

The subsequent mechanistic study compared the different responses of A549 and SK-MES-1 cells toward quartz particles of respirable size. The SK-MES-1 cells demonstrate typical apoptotic morphological changes after quartz exposure and cell cycle analysis by flow cytometry further shows dose-responsive formation of sub-G1 peak. The administration of pan-caspase inhibitor protects SK-MES-1 cells from death; this

demonstrates the possible role of caspase in quartz-induced cell death. The mitochondrial membrane potential assay shows that the mitochondria damage and decrease of mitochondrial membrane potential is an early event in quartz-induced cell death. The results from the A549 cells indicate that quartz-induced A549 cell death is likely due to necrosis.

Apoptosis has been suggested to be one of the essential underlying mechanisms of pulmonary fibrosis by many studies. SK-MES-1 cells are type I-like alveolar cells and A549 cells are type II-like alveolar cells; it is reasonable to speculate that quartz may induce apoptosis in type I alveolar cells, which would lead to pulmonary fibrosis, the typical pathological change of silicosis. Our study may contribute to further understanding of the mechanisms of silicosis.

The successful testing of air particulates demonstrates the potential application of the RT-PCR technique for biomonitoring of air quality. For example, one of the potential applications of the RT-CES technique is to evaluate the cytotoxicity of various fractions of air samples based on size for environmental assessment. We could use the cytotoxicity information to direct further investigation into toxic components in the mixture of particulate matter using advanced analytical techniques such as mass spectrometry. Such studies will help industry and government to prioritize their effort and money to relatively potent components of particulate matter and provide useful information on the regulation of air pollutants.